PL-TR-96-2250

THE DEPENDENCE OF MAGNITUDE UNCERTAINTY ON STATION COVERAGE

Steven Bottone
Mark D. Fisk
Henry L. Gray
Gary D. McCartor

Mission Research Corporation
735 State Street
PO Drawer 719
Santa Barbara, CA 93102-0719

31 August 1996

Scientific Report No. 1

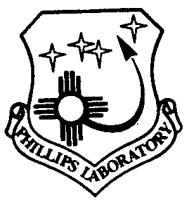

PHILLIPS LABORATORY
Directorate of Geophysics
AIR FORCE MATERIEL COMMAND
HANSCOM AFB, MA 01731-3010

SPONSORED BY
Advanced Research Projects Agency (DoD)
Nuclear Monitoring Research Office
ARPA ORDER No. 0325

MONITORED BY
Phillips Laboratory
CONTRACT No. F19628-95-C-0101

The views and conclusions contained in this document are those of the authors and should not be interpreted as representing the official policies, either express or implied, of the Air Force or U.S. Government.

This technical report has been reviewed and is approved for publication.

DELAINE R. REITER
Contract Manager
Earth Sciences Division

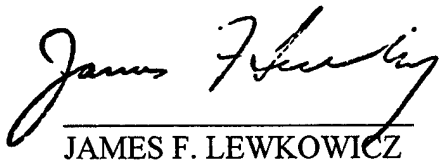

JAMES F. LEWKOWICZ
Director
Earth Sciences Division

This report has been reviewed by the ESD Public Affairs Office (PA) and is releasable to the National Technical Information Service (NTIS).

Qualified requestors may obtain copies from the Defense Technical Information Center. All others should apply to the National Technical Information Service.

If your address has changed, or you wish to be removed from the mailing list, or if the addressee is no longer employed by your organization, please notify PL/IM, 29 Randolph Road, Hanscom AFB, MA 01731-3010. This will assist us in maintaining a current mailing list.

Do not return copies of this report unless contractual obligations or notices on a specific document requires that it be returned.

REPORT DOCUMENTATION PAGE

Form Approved
OMB NO. 0704.0188

1. AGENCY USE ONLY *(Leave Blank)*	2. REPORT DATE	3. REPORT TYPE AND DATES COVERED
	31 Aug 1996	Scientific Report No. 1

4. TITLE AND SUBTITLE
The Dependence of Magnitude Uncertainty on Station Coverage

5. FUNDING NUMBERS
Contract F19628-95-C-0101
PE 62301E
PR NM95 TA GM WU AA

6. AUTHOR(s)
Steven Bottone
Mark D. Fisk
Henry L. Gray
Gary D. McCartor*

7. PERFORMING ORGANIZATION NAME(S) AND ADDRESS(ES)
Mission Research Corporation
735 State Street, P. O. Drawer 719
Santa Barbara, CA 93102-0719

8. PERFORMING ORGANIZATION REPORT NUMBER
MRC-R-1527

9. SPONSORING/MONITORING AGENCY NAME(S) AND ADDRESS(ES)
Phillips Laboratory
29 Randolph Road
Hanscom Air Force Base, MA 01731-3010
Contract Manager: Delaine Reiter/GPE

10. SPONSORING/MONITORING AGENCY REPORT NUMBER
PL-TR-96-2250

11. SUPPLEMENTARY NOTES
* Department of Physics, Southern Methodist University, Dallas, TX
This research was partially supported under contract F19628-95-C-0098 with Southern Methodist University.

12a. DISTRIBUTION/AVAILABILITY STATEMENT
Approved for public distribution;
distribution unlimited

12b. DISTRIBUTION CODE

13. ABSTRACT *(Maximum 200 words)*

A useful event characterization parameter for relatively large (e.g., mb > 4) teleseismic events is mb–Ms, provided the events are not too deep. To use mb–Ms as a parameter with which to "screen" events of natural seismicity, at a given confidence level, the uncertainty (standard deviation) in mb–Ms must be quantified. This report presents a generalization to the current method of screening events using mb–Ms by including correlation between station observations due to station coverage. After a description of the current method used to estimate the uncertainty in mb–Ms, an analysis is presented, using all events currently available in the Reviewed Event Bulletin (REB) for which Ms was measured at six or more stations, to determine the dependence on station coverage. Generally, Ms measurements at stations which are located along the same direction from the event are positively correlated, while measurements at stations which are located at near right angles from the event are negatively correlated. Using the data to estimate the correlation between stations as a function of angle relative to the event location, a multivariate statistical model for the uncertainty in mb–Ms is given and applied to each of the 400 relevant events in the REB. An interpretation of the results and recommendations for treatment of station coverage is provided.

14. SUBJECT TERMS		15. NUMBER OF PAGES
Seismic Event Characterization	Comprehensive Test Ban	42
Magnitude Uncertainty	Station Coverage	16. PRICE CODE
Multivariate Statistical Analysis	Reviewed Event Bulletin	

17. Security CLASSIFICATION OF REPORT	18. Security CLASSIFICATION OF THIS PAGE	19. Security CLASSIFICATION OF ABSTRACT	20. LIMITATION OF ABSTRACT
UNCLASSIFIED	UNCLASSIFIED	UNCLASSIFIED	SAR

NSN 7540-01-280-5500

Standard Form 298 (Rev. 2-89)
Prescribed by ANSI Std. 239-18
298-102

CLASSIFIED BY:

DECLASSIFY ON:

Table of Contents

1. Intoduction 1
1.1. Current Method for Computing Magnitude Uncertainty 1
2. Data Analysis 4
2.1. Data 4
2.2. Station Corrections 5
2.3. Definition of Station Coverage 5
2.4. Magnitude Uncertainty (uncorrected) 9
2.5. Correcting for Finite-Sized Samples 13
2.6. Magnitude Uncertainty (corrected) 15
3. Multivariate Approach 22
3.1. Uncertainty in mb–Ms Using Multivariate Statistical Analysis 22
3.2. The Correlation Coefficient 24
3.3. The Consistency of the Correlation Coefficient Function 25
3.4. Results 28
4. Conclusions and Recommendations 30
5. References 31

List of Figures

1. Mapping of event and station locations from spherical earth to $x'y'$ Cartesian plane. . . 6

2. Coverage for one station, equal to $\beta/2\pi = 1/N$ 7

3. Scatterplot of Ms magnitude uncertainty versus station coverage for 2 station subsets, $A = 360°$ 10

4. Ms magnitude uncertainty versus station coverage for 2 station subsets, $A = 360°$ (uncorrected). 11

5. Ms magnitude uncertainty versus station coverage for 2 station subsets, $A = 180°$ (uncorrected). 12

6. Ms magnitude uncertainty versus station coverage for 2 station subsets, $A = 90°$ (uncorrected). 13

7. Ms magnitude uncertainty versus station coverage for 2 station subsets, $A = 360°$ (corrected). 16

8. Ms magnitude uncertainty versus station coverage for 3 station subsets, $A = 360°$ (corrected). 16

9. Ms magnitude uncertainty versus station coverage for 4 station subsets, $A = 360°$ (corrected). 17

10. Ms magnitude uncertainty versus station coverage for 5 station subsets, $A = 360°$ (corrected). 17

11. Ms magnitude uncertainty times the square root of number of stations versus station coverage for $n = 1, 2, 3.4, 5$, $A = 360°$ (corrected). 18

12. Ms magnitude uncertainty versus station coverage for $n = 1, 2, 3.4, 5$, $A = 360°$ (corrected). 19

13. Ms magnitude uncertainty versus station coverage for $n = 1, 2, 3.4, 5$, $A = 180°$ (corrected). 20

14. mb magnitude uncertainty versus station coverage for $n = 1, 2, 3.4, 5$, $A = 360°$ (corrected). 21

15. mb magnitude uncertainty versus station coverage for $n = 1, 2, 3.4, 5$, $A = 180°$ (corrected). 21

16. Correlation coefficient as a function of cosine of the station angle for 2 station subsets and smooth fit. 25

17. Left-hand side of Eq (59) for n even and Eq (60) for n odd versus n. 28

1. Introduction

A useful event characterization parameter for relatively large (e.g., mb > 4) teleseismic events is mb–Ms (e.g., Marshall and Basham, 1972; Blandford et al., 1992), provided the events are not too deep. To use mb–Ms as a parameter with which to "screen" events of natural seismicity, at a given confidence level, the uncertainties of these measurements must be quantified. Currently, our treatment of the uncertainty in mb–Ms (e.g., Fisk et al., 1995), employed by event screening tools available on the World Wide Web site at the Prototype International Data Center, Arlington, VA, assumes that the standard deviations for individual mb and Ms measurements are 0.3 magnitude units. The uncertainties are due to numerous factors, including near-source, path, station, radiation pattern and random scattering effects. Many of these factors are systematic in nature and can be corrected if enough information is available, as discussed by Rautian and Khalturin (1994). Systematic errors due to radiation pattern effects are described by von Seggern (1970).[1]

Our current approach for estimating the uncertainty in mb-Ms further depends on the number of observing stations, but does not explicitly account for correlations between station measurements, which are due, at least in part, to radiation pattern effects. In this report, we present a generalization to our current approach by including correlation between stations due to station coverage. Station coverage, to be defined below, is essentially how much azimuthal angular coverage the stations make about the event location. This effect presumably depends on the radiation pattern of the propagating seismic wave, although it is not necessarily the case that such an effect can be seen in the data. The methods presented below to treat mb–Ms uncertainty due to station coverage should be applied in computing the overall mb–Ms uncertainty after all known corrections for systematic errors have been made. A similar approach that treats station correlation for mb measurements as a function of distance on the focal sphere is presented in McLaughlin, et al. (1988).

In the remainder of Section 1, we describe our current method of computing a confidence interval for mb–Ms. In Section 2, we describe the data set used to estimate the magnitude uncertainties, based on all events in the Reviewed Event Bulletin (REB) for which Ms was measured at six or more stations. In Section 2, we also describe corrections for station bias, a definition of station coverage, and estimates of the standard deviations of mb and Ms. In Section 3, we present the multivariate statistical treatment of the uncertainty in mb-Ms due to station coverage. In Section 4, we provide conclusions and recommendations as to the treatment of the uncertainty in mb-Ms.

1. Such corrections are being pursued by the Magnitude Panel (Murphy et al.), established by the Nuclear Treaty Programs Office. We plan to adopt the procedures established by the Magnitude Panel once available.

1.1. Current Method for Computing Magnitude Uncertainty

In the current version of the event characterization software, installed at the Center for Monitoring Research (CMR), an event retrieved from the Reviewed Event Bulletin (REB) database is tested using mb–Ms in the following way. (A test for focal depth is also applied in conjunction, but is not discussed here.) For an event for which there are both mb and Ms magnitude measurements, let N_b be the number of stations (*nsta* in the schema) with mb measurements. The network average of mb, $\overline{m}_b$, is given by the sample mean of the N_b data values,

$$\overline{m}_b = \frac{1}{N_b} \sum_{j=1}^{N_b} m_{b,j} \ , \tag{1}$$

where the sum is over all stations, j, measuring mb. The network average of Ms, $\overline{M}_s$, is computed in a slightly more complicated manner (Jepsen, 1996). The value of *nsta* given in the REB is the total number of array elements measuring Ms. For a given station, j, let n_j be the number of elements which measured Ms, so that

$$\text{nsta} = \sum_{j=1}^{N_s} n_j \ , \tag{2}$$

where N_s is the total number of stations measuring Ms. The station average, $M_{s,j}$, is given by the sample mean of the n_j values of Ms at station j, and the network average of Ms is then given by the sample mean of the N_s values of $M_{s,j}$,

$$\overline{M}_s = \frac{1}{N_s} \sum_{j=1}^{N_s} M_{s,j} \ . \tag{3}$$

The network average for mb–Ms is then taken to be $\overline{m}_b - \overline{M}_s$. A $100(1-\alpha)\%$ confidence interval, usually taken to be 99% ($\alpha = 0.01$), about the expected value of mb–Ms is then compared with 1.2. If this confidence interval is entirely below 1.2 (entirely outside the nuclear explosion population), that is, if the largest value of the confidence interval is less than 1.2, then the event is considered earthquakelike and screened. The confidence interval for mb–Ms is determined as follows.

The uncertainty (standard deviation) for both individual mb and Ms measurements, independent of the value of mb or Ms, is taken to be 0.3. This corresponds to a variance for both of 0.09, that is,

$$\sigma_b^2 = \sigma_s^2 = (0.3)^2 = 0.09 . \quad (4)$$

The variance of the mean of N_b independent measurements of mb is given by σ_b^2/N_b with a similar expression for Ms. The variance of $\overline{m}_b - \overline{M}_s$, denoted by σ^2, under the assumption that mb and Ms measurements are uncorrelated, is

$$\sigma^2 = \text{variance}(\overline{m}_b - \overline{M}_s) = \frac{\sigma_b^2}{N_b} + \frac{\sigma_s^2}{N_s} . \quad (5)$$

The $100(1-\alpha)\%$ confidence interval for $\overline{m}_b - \overline{M}_s$ is determined by assuming that this quantity is a normally distributed random variable with variance σ^2 with a true (unknown) mean equal to $\mu_b - \mu_s$. Let x_α be defined such that $\text{Prob}(x > x_\alpha) = \alpha$ for x distributed as normal with zero mean and unit variance. Then

$$\text{Prob}(\mu_b - \mu_s < \overline{m}_b - \overline{M}_s + x_\alpha \sigma) = 1 - \alpha \quad (6)$$

and the one-sided $100(1-\alpha)\%$ confidence interval for $\mu_b - \mu_s$ is $(-\infty, \overline{m}_b - \overline{M}_s + x_\alpha \sigma]$. Therefore, an event with measured $\overline{m}_b - \overline{M}_s$ is screened if

$$\overline{m}_b - \overline{M}_s + x_\alpha \sigma < 1.2 \ . \quad (7)$$

(Using a two-sided $100(1-\alpha)\%$ confidence interval, $[\overline{m}_b - \overline{M}_s - x_{\alpha/2}\sigma, \overline{m}_b - \overline{M}_s + x_{\alpha/2}\sigma]$, the screening criterion is $\overline{m}_b - \overline{M}_s + x_{\alpha/2}\sigma < 1.2$.)

Before showing how this magnitude uncertainty can be generalized to include correlation due to station coverage, we must examine the REB database to see if there actually is such correlation.

2. Data Analysis

Before describing a method which will generalize the mb–Ms magnitude uncertainty calculation it is necessary to examine the available REB data to determine if, indeed, there is some dependence in the variance of the magnitudes on station coverage. An appropriate definition of station coverage will be given below.

2.1. Data

For the purpose of studying the effect of station coverage on magnitude uncertainty we use all events in the REB for which there are more than six Ms measurements available. There were 400 such events, dated from 11 Jan 1995 (1995011) to 2 Jun 1996 (1996154). Those events which fell between the dates 17 Jan 1996 (1996017) and 21 Feb 1996 (1996052) were not used due to an erroneous formula used to calculate Ms (Israelsson, 1996). There were 116 stations in this list of data. Some of the stations consist of multiple array elements each of which may measure Ms and these individual array element measurements are what is reported in the *stamag* table. The total number of array elements measuring Ms is the number, *nsta*, which is reported in the *netmag* table, and not the total number of stations with Ms measurements. The network average Ms, reported in the *origin* and *netmag* tables, average over stations and not elements and, therefore, is not computed by summing the entries in the *stamag* table and dividing by *nsta* (see Eq (3) above for the correct formula). The total number of array elements in the list is 141.

For each event, i, the sample mean for mb and Ms can be computed as in Eq (1) and (3). The residual for a given mb measurement for event i at station j is given by

$$e_{b,ij} = m_{b,ij} - \overline{m}_{b,i}, \qquad j = 1, \ldots, N_{b,i}, \tag{8}$$

where $m_{b,ij}$ is the mb magnitude for event i at station j and $N_{b,i}$ is the number of mb measurements for event i. The residuals for Ms measurements are given in a similar way. The maximum likelihood estimate (MLE) of the variance based on all mb measurements is given by

$$s_b^2 = \left[\left(\sum_{i=1}^{N_e} N_{b,i}\right)\right]^{-1} \sum_{i=1}^{N_e} \sum_{j=1}^{N_{b,i}} e_{b,ij}^2 \ , \tag{9}$$

with a similar definition for s_s^2. Note that this definition is simply summing the residuals for all measurements and dividing by the total number of measurements, which is sensible only if it is being assumed that the variance of mb (and Ms) measurements is independent of magnitude

(independent of event). When Eq (9) (and the appropriate equation for Ms) are applied to the 400 selected events they give

$$s_b = 0.38, \qquad s_s = 0.26. \tag{10}$$

The unbiased sample standard deviations for mb and Ms, which are obtained by subtracting N_e in the denominator of Eq (9), are $s_b = 0.39$ and $s_s = 0.28$.

2.2. Station Corrections

It is often the case that a given station will give magnitude readings that are systematically greater or less than the network average due to local geophysical properties and this systematic error accounts for some of the variance in magnitude measurements. This problem is currently being addressed by Keith McLaughlin of S-Cubed (McLaughlin, 1996) and once he publishes his list of station corrections, we will incorporate them into the Custom Event Characterization Run. For now, we will estimate station bias using the 400 selected events from the REB. We define the bias at station j, b_j, one for mb and one for Ms, by

$$b_j = \frac{1}{N_j} \sum_i (m_{ij} - \bar{m}_i), \tag{11}$$

where the sum is over those events, total number equal to N_j, which were observed at station j. A corrected magnitude measure at station j, one for mb and one for Ms, is then given by

$$m_{j,\,\text{corrected}} = m_{j,\,\text{uncorrected}} - b_j. \tag{12}$$

Using corrected values for mb and Ms in Eq (9) (and the appropriate equation for Ms), the variances are lowered somewhat. The results for the 400 selected events are

$$s_b = 0.33, \quad s_s = 0.23 \quad \text{(MLE)}; \qquad s_b = 0.34, \quad s_s = 0.25 \quad \text{(unbiased variance)}. \tag{13}$$

2.3. Definition of Station Coverage

Let an event located at latitude λ_e and longitude ϕ_e be observed, by mb or Ms, at N stations with latitudes λ_j and longitudes ϕ_j, $j = 1, \ldots, N$. We wish to define a number q, called the station coverage, with q between $1/N$ and one, such that q near one corresponds to the N stations

being in directions that are spread uniformly about the event location and q near $1/N$ corresponds to the stations all in the same direction. It is easier to work in a flat $x'y'$ plane than on a sphere so we map the event location to the origin of the $x'y'$ plane and the N station locations to points on the unit circle about the origin, with station one on the x' axis. This transformation, T: $(\lambda, \phi) \rightarrow (x', y')$, is shown in Figure 1.

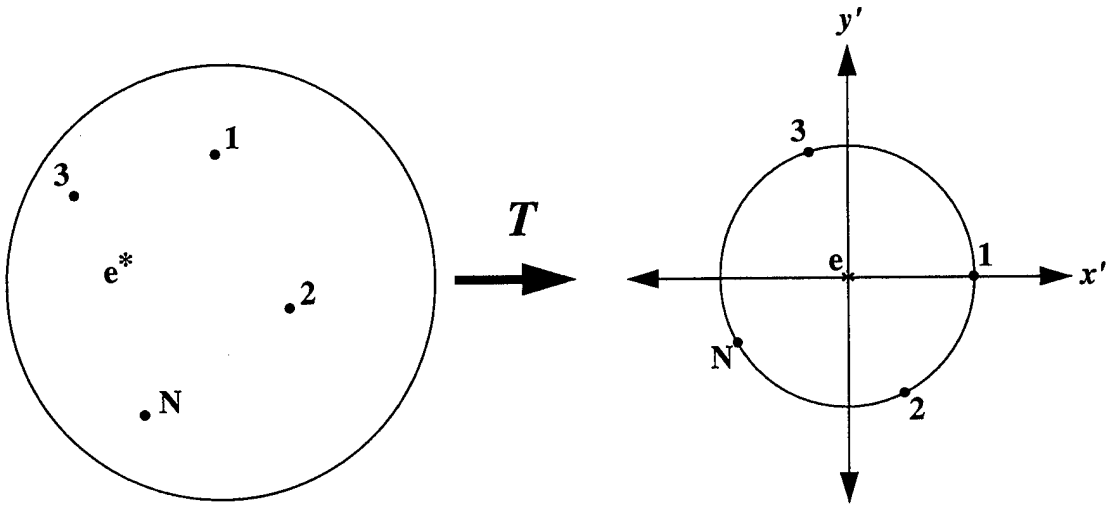

Figure 1. Mapping of event and station locations from spherical earth to $x'y'$ Cartesian plane.

To carry out this transformation let $\hat{\mathbf{x}}_e$ be a unit vector in the direction from the earth's center to the location on the earth's surface of the event. In a right-handed Cartesian coordinate system with origin at the earth's center, z axis through the north pole, and x axis through zero degrees longitude, this vector is

$$\hat{\mathbf{x}}_e = \cos\lambda_e \cos\phi_e \hat{\mathbf{e}}_x + \cos\lambda_e \sin\phi_e \hat{\mathbf{e}}_y + \sin\lambda_e \hat{\mathbf{e}}_z, \tag{14}$$

where $\hat{\mathbf{e}}_x$, $\hat{\mathbf{e}}_y$, and $\hat{\mathbf{e}}_z$ are unit vectors along the x, y and z axes, respectively. Similarly,

$$\hat{\mathbf{x}}_j = \cos\lambda_j \cos\phi_j \hat{\mathbf{e}}_x + \cos\lambda_j \sin\phi_j \hat{\mathbf{e}}_y + \sin\lambda_j \hat{\mathbf{e}}_z, \qquad j = 1, \ldots, N, \tag{15}$$

is a unit vector in the direction of station j. A plane containing the origin, the event location, and station j, has a unit normal, $\hat{\mathbf{n}}_j$, perpendicular to both $\hat{\mathbf{x}}_e$ and $\hat{\mathbf{x}}_j$, given by

$$\hat{\mathbf{n}}_j = \frac{\hat{\mathbf{x}}_j \times \hat{\mathbf{x}}_e}{|\hat{\mathbf{x}}_j \times \hat{\mathbf{x}}_e|}, \qquad j = 1, \ldots, N. \tag{16}$$

All such vectors are in the plane normal to $\hat{\mathbf{x}}_e$. The angle made by two great circles through the event location and two stations is, by definition, the angle made by the two planes containing the origin, the event location, and the station locations, or, equivalently, the angle made by the normals to these planes. A primed coordinate system can be introduced in the plane normal to $\hat{\mathbf{x}}_e$ by setting the unit vector along the x' axis, $\hat{\mathbf{e}}'_x$, equal to $\hat{\mathbf{n}}_1$, and the unit vector along the y' axis, $\hat{\mathbf{e}}'_y$, equal to a vector perpendicular to both $\hat{\mathbf{x}}_e$ and $\hat{\mathbf{e}}'_x$, that is,

$$\hat{\mathbf{e}}'_x = \hat{\mathbf{n}}_1, \qquad \hat{\mathbf{e}}'_y = \hat{\mathbf{x}}_e \times \hat{\mathbf{e}}'_x . \tag{17}$$

In this coordinate system, the points with coordinates

$$x'_j = \hat{\mathbf{n}}_j \cdot \hat{\mathbf{e}}'_x, \qquad y'_j = \hat{\mathbf{n}}_j \cdot \hat{\mathbf{e}}'_y, \qquad j = 1, \ldots, N, \tag{18}$$

are points on the unit circle with point 1 on the x' axis, as in Figure 1.

Consider point j on the unit circle of the $x'y'$ plane, which makes an angle α_j with the x' axis ($\alpha_1 = 0$). The sector from $\alpha_j - \beta/2$ to $\alpha_j + \beta/2$, as shown in Figure 2, has total angle β.

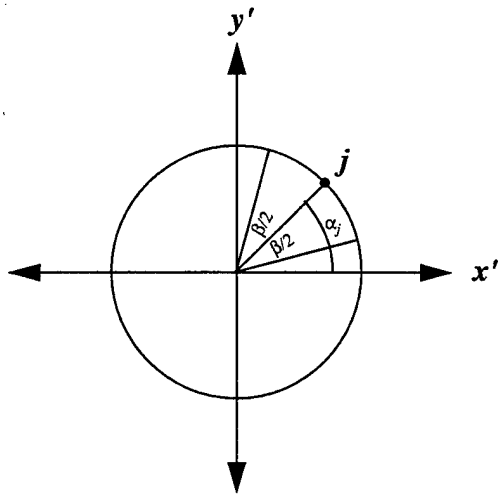

Figure 2. Coverage for one station, equal to $\beta/2\pi = 1/N$.

The fraction of the total angle, $A = 2\pi$, covered by the angular sector of size β, is β/A. The interval defined by

$$I_j = [a_j, b_j], \tag{19}$$

where

$$a_j = \frac{1}{A}\left(\alpha_j - \frac{\beta}{2}\right), \qquad b_j = \frac{1}{A}\left(\alpha_j + \frac{\beta}{2}\right), \tag{20}$$

has measure, $\mu(I_j) = \beta/A$, which is less than or equal to one for $\beta \le A$.

Now consider all the intervals, $I_j = [a_j, b_j]$, $j = 1, \ldots, N$. If the interval, I_j, is such that either $a_j < 0$ or $b_j > 1$, then split the interval into two intervals, $I_j = I_j^{(1)} \cup I_j^{(2)}$, where

$$I_j^{(1)} = [0, b_j], \qquad I_j^{(2)} = [1 + a_j, 1], \qquad \text{if } a_j < 0, \tag{21}$$

$$I_j^{(1)} = [0, b_j - 1], \qquad I_j^{(2)} = [a_j, 1], \qquad \text{if } b_j > 1, \tag{22}$$

so that all intervals are in $[0, 1]$. We then define the coverage, q, of N stations to be

$$q = \mu\left(\bigcup_{j=1}^{N} I_j\right). \tag{23}$$

It is readily seen that this definition yields a number between β/A and one. If β is chosen to be A/N, then $q = 1$ if and only if the N points are equally spaced on the unit circle, and $q = 1/N$, the smallest possible value, if and only if all stations are located at the same angle. For example, if $N = 4$ and the stations are located at $0°$, $90°$, $180°$, and $270°$, then $q = 1$; if all the stations are located at $0°$, then $q = 0.25$; if two stations are at $0°$ and two stations are at $135°$, then $q = 0.50$; and so on.

If it were suspected that the observed radiation pattern for the magnitude measurements had some symmetry, then it might be useful to choose A to be something other than $360°$ in the definition of station coverage. For example, if the radiation pattern is two-leafed, i.e., symmetric about some axis, then the magnitudes at points $180°$ apart would be the same (all other things being equal) and so the coverage might more usefully be defined by setting $A = 180°$, which considers intervals separated by $180°$ to be the same. If a four-leafed radiation is expected, then $A = 90°$ might be more useful. The usefulness of choosing A to be something other than $360°$ for the actual data will be examined below.

2.4. Magnitude Uncertainty (uncorrected)

To study the effect of station coverage on magnitude uncertainty we examine the residuals of subsets of the data (the difference between the mean for the subset and the mean for the entire set) as a function of station coverage, q. For a given event, i, let N_i be the number of station measurements available (for either mb or Ms) and let $\overline{m}_i$ be the sample mean as computed by Eq (1) (for mb) or Eq (3) (for Ms). Consider all subsets of the N_i stations taken n at a time. The total number of such subsets is

$$\binom{N_i}{n} = \frac{N_i!}{n!(N_i-n)!}. \tag{24}$$

For example, if $N_i = 5$ and $n = 2$ then there are 10 subsets, namely, {1,2}, {1,3}, {1,4}, {1,5}, {2,3}, {2,4}, {2,5}, {3,4}, {3,5}, and {4,5}. For a given subset, $\{j_1, \ldots, j_n\}$, denote the sample mean relative to that subset by

$$\overline{m}_i(j_1, \ldots, j_n) = \frac{1}{n}(m_{i,j_1} + \ldots + m_{i,j_n}), \qquad 1 \le j_1 < \ldots < j_n \le N_i. \tag{25}$$

The residual for each subset is given by

$$e_i(j_1, \ldots, j_n) = \overline{m}_i(j_1, \ldots, j_n) - \overline{m}_i, \qquad 1 \le j_1 < \ldots < j_n \le N_i. \tag{26}$$

Each subset, $\{j_1, \ldots, j_n\}$, $1 \le j_1 < \ldots < j_n \le N_i$, consists of n stations surrounding the event location with a corresponding station coverage, q, computed using Eq (23). In studying the relation of magnitude uncertainty and station coverage it would, of course, be better to use the true mean rather than the sample mean in Eq (26), but the true mean is not known. How this affects the calculations will be discussed below.

We are now in a position to determine if there is any dependence of uncertainty on station coverage. Figure 3 is a scatterplot of the square root of the square (absolute value) of the residuals of Ms measurements for all subsets of two stations for every event in the database satisfying the conditions that the number of Ms stations for each event is greater than six and the station coverage for all $N_{s,i}$ stations used to compute $\overline{m}_{s,i}$ is greater than 0.6. No symmetry is assumed at this point so A is chosen to be equal to $360°$.

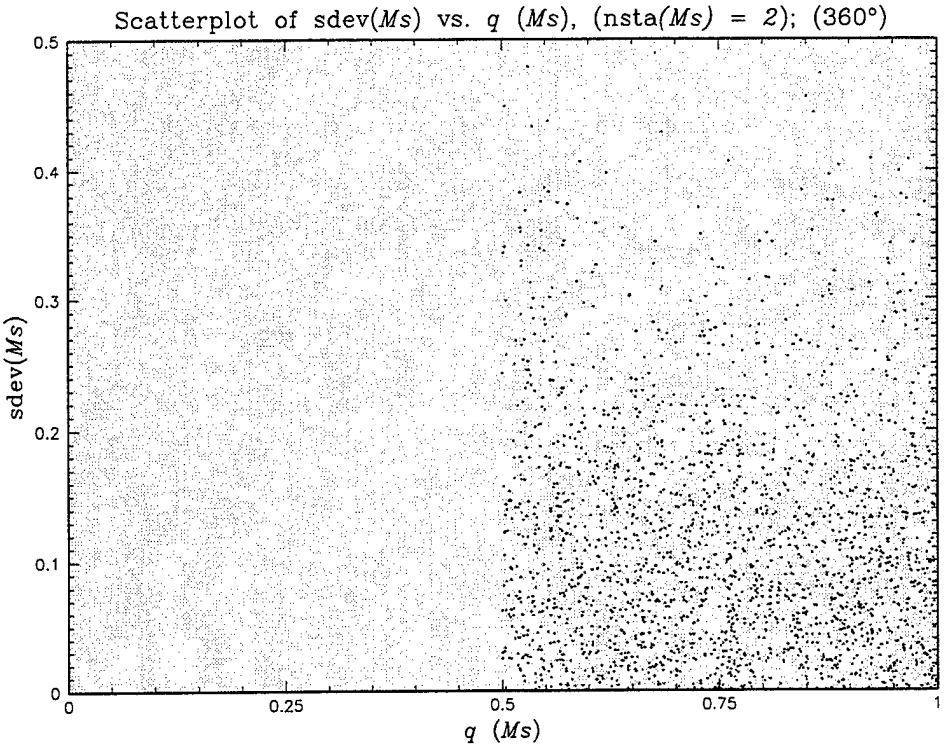

Figure 3. Scatterplot of Ms magnitude uncertainty versus station coverage for 2 station subsets, $A = 360°$.

One can see from Figure 3 that the station coverage varies from $q = 1/n = 0.50$ to $q = 1$. It is difficult to tell from this scatterplot if there is any dependence on q. To aid seeing if there is some dependence on q, we compute the average variance of the data as a function of q. To do this we separate the data into K bins, $q_k < q < q_{k+1}$, $k = 1, \ldots, K$, with $1/n = q_1 < \ldots < q_{K+1} = 1$. The sample variance for subsets of size n in bin k is

$$s^2_{n,k} = \frac{1}{N_{n,k}} \sum_{i=1}^{N_e} \sum_{\substack{1 \le j_1 < \ldots < j_n \le N_i \\ q_k < q < q_{k+1}}} e(j_1, \ldots, j_n)^2, \tag{27}$$

where N_e is the total number of events, the second sum is restricted to subsets with q in bin k, and $N_{n,k}$ is the total number of terms in the entire summation. Figure 4 contains a plot of $s_{2,k}$, $k = 1, \ldots, 5$, with bins [0.5,0.6], [0.6,0.7],..., [0.9,1.0]. Each $s_{n,k}$ is plotted at the midpoint of its respective bin. The error bars are computed by assuming the $s^2_{n,k}$ are distributed as chi-square with $N_{n,k}$ degrees of freedom and choosing a 95% confidence interval, which is chosen to be

$$[N_{n,k} s^2_{n,k} / \chi^2_{0.025}, N_{n,k} s^2_{n,k} / \chi^2_{0.975}]. \tag{28}$$

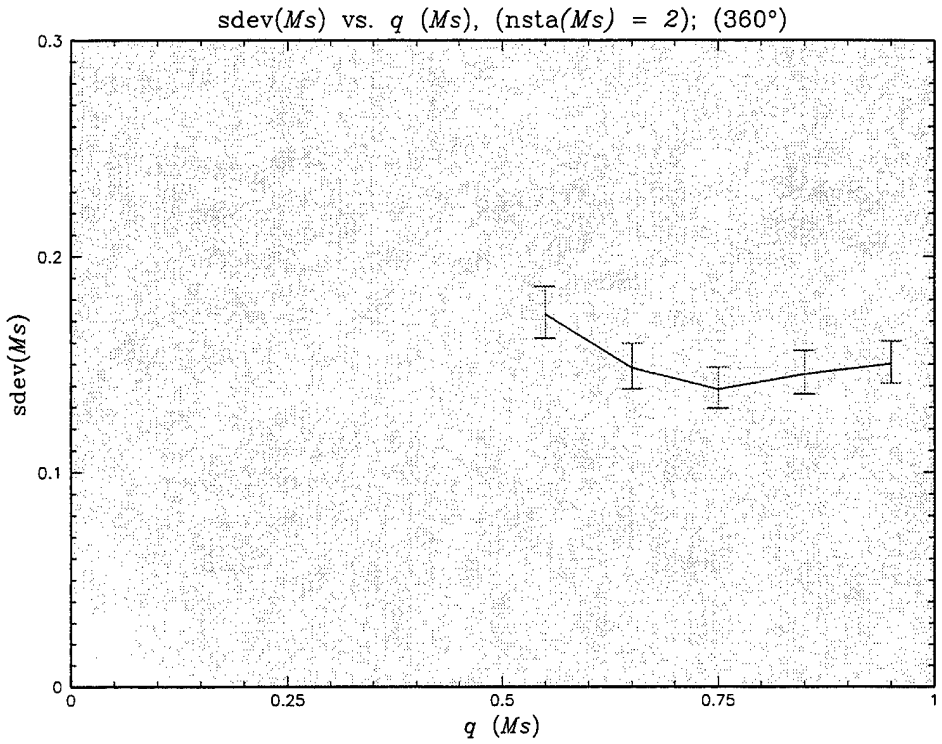

Figure 4. Ms magnitude uncertainty versus station coverage for 2 station subsets, $A = 360°$ (uncorrected).

Figure 4 shows a dependence on q which has a maximum at $q = 0.50$, has a minimum near $q = 0.75$, and increases a q approaches one but not to the maximum value. For $n = 2$ stations, $q = 0.50$ corresponds to stations at the same angle, $q = 0.75$ corresponds to stations separated by 90 degrees and $q = 1$ corresponds to stations separated by 180 degrees. It is seen, then, that the greatest uncertainty occurs when two stations are in the same direction from the event. This implies that Ms magnitude measurements from stations in the same direction are positively correlated. Minimum uncertainty, which implies a negative correlation, occurs when stations are separated by 90 degrees. Stations separated by 180 degrees show more uncertainty, more correlation, than those separated by 90 degrees but less than those separated by 0 degrees. This suggests that there may be a radiation pattern with a 180 degree symmetry. This should be observed if we take $A = 180°$ in our definition of station coverage, q, and, as Figure 5 shows, there is a monotonic decrease of magnitude uncertainty with increasing q.

In Figure 5, $q = 0.50$ corresponds to stations separated by either 0 degrees or 180 degrees, while $q = 1$ corresponds to separations of 90 degrees. If there were a prominent four-leafed radiation pattern there would be a minimum at $q = 0.75$, corresponding to stations separated by either 45

degrees or 135 degrees, which is not the case. A plot with $A = 90°$, which is shown in Figure 6, does not display a monotonic decrease in uncertainty with q, which would be the case if there were prominent four-leaf radiation patterns present in the Ms magnitude data.

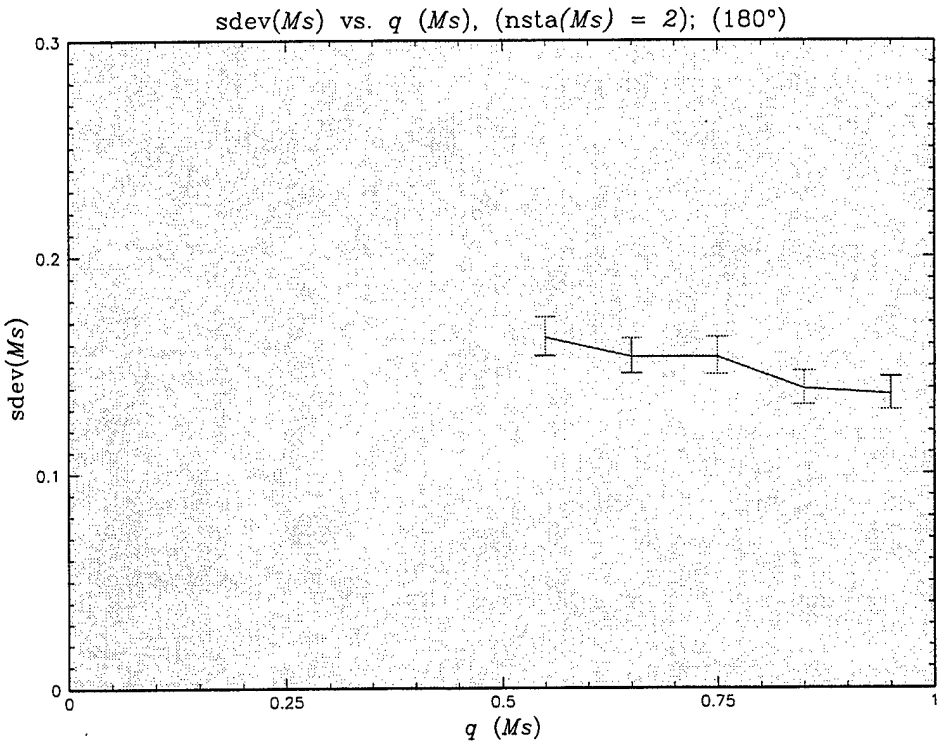

Figure 5. Ms magnitude uncertainty versus station coverage for 2 station subsets, $A = 180°$ (uncorrected).

Before discussing the relation between magnitude uncertainty and station coverage for more than two stations and for mb magnitude data, it is necessary to examine the effect on these calculations of using finite-sized data samples, and making any necessary corrections. The square root of the variance of all data in Figure 3 is 0.15. Since these variances were computed using two station combinations, one would expect, if there were no correlation in the data, for the variance for two stations to be equal to the variance for one station divided by two. Or, equivalently, the square root of two times 0.15, which is 0.21, should be equal to the square root of the single station value, s_s, given in Eq (13) (we are using data corrected for station bias, here).

This value is 0.23, slightly higher than 0.21. This would not be alarming in itself, but as we shall see, as the number of elements increase in the stations subsets, the difference between n times the

single station variance and the computed variance increases with n, which is due to the use of finite-sized samples. We will now show how to correct the variance for finite-sized samples.

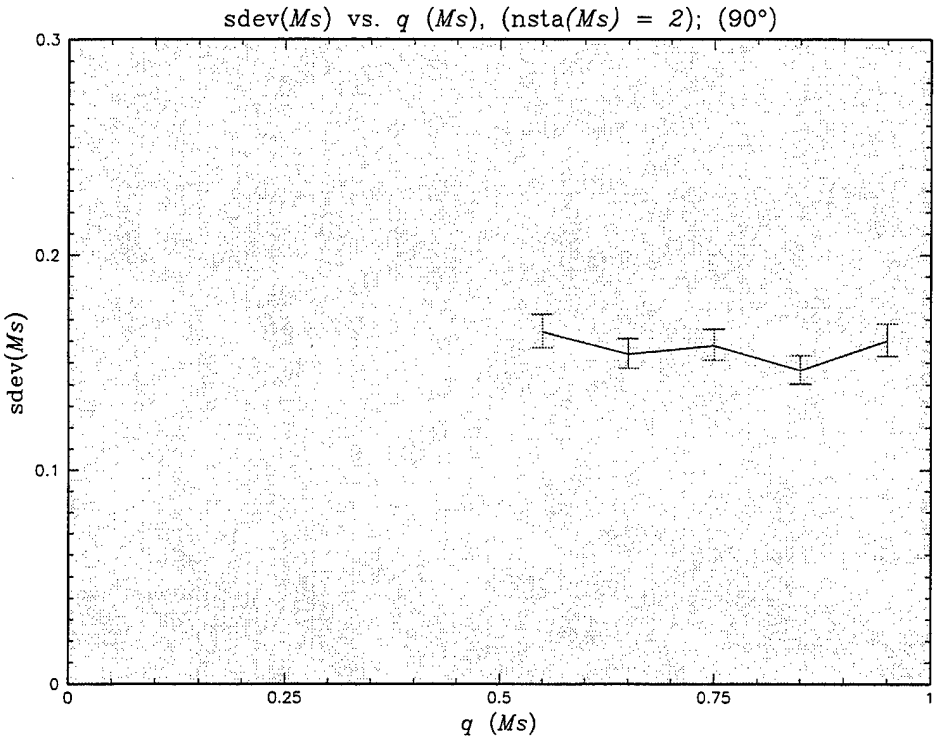

Figure 6. Ms magnitude uncertainty versus station coverage for 2 station subsets, $A = 90°$ (uncorrected).

2.5. Correcting for Finite-Sized Samples

Consider a data sample of size N, $\{x_j; j = 1, \ldots, N\}$. The sample mean, as usual, is given by

$$\bar{x} = \frac{1}{N} \sum_{j=1}^{N} x_j \ . \tag{29}$$

Define the sample variance over all subsets of size n, s_n^2, by

$$s_n^2 = \frac{n!(N-n)!}{N!} \sum_{1 \le j_1 < \ldots < j_n \le N} \left[\frac{1}{n}(x_{j_1} + \ldots + x_{j_n}) - \bar{x} \right]^2, \qquad 1 \le n \le N. \tag{30}$$

For $n = 1$, this sum reduces to

$$s_1^2 = \frac{1}{N}\sum_{j=1}^{N}(x_j-\bar{x})^2 , \tag{31}$$

which is the usual maximum likelihood estimate of the variance. Eq (30) may be rewritten

$$\begin{aligned} s_n^2 &= \frac{(N-n)!}{N!}\sum_{j_1\neq\ldots\neq j_n=1}^{N}\left[\frac{x_{j_1}-\bar{x}}{n}+\ldots+\frac{x_{j_n}-\bar{x}}{n}\right]^2 \\ &= \frac{(N-n)!}{N!}\frac{1}{n^2}\sum_{j_1\neq\ldots\neq j_n=1}^{N}\left[(x_{j_1}-\bar{x})^2+\ldots+(x_{j_n}-\bar{x})^2+2(x_{j_1}-\bar{x})(x_{j_2}-\bar{x})+\ldots\right]. \end{aligned} \tag{32}$$

Each of the n squared terms in the square brackets gives

$$\sum_{j_1\neq\ldots\neq j_n=1}^{N}(x_{j_k}-\bar{x})^2 = \frac{(N-1)!}{(N-n)!}\sum_{j=1}^{N}(x_j-\bar{x})^2, \qquad k = 1,\ldots,n, \tag{33}$$

and each of the $n(n-1)/2$ remaining cross terms gives

$$\sum_{j_1\neq\ldots\neq j_n=1}^{N}2(x_{j_k}-\bar{x})(x_{j_m}-\bar{x}) = \frac{(N-2)!}{(N-n)!}\sum_{i\neq j=1}^{N}2(x_i-\bar{x})(x_j-\bar{x}), \quad 1\le k<m\le n. \tag{34}$$

Eq (32) now becomes

$$s_n^2 = \frac{1}{n}\frac{1}{N}\sum_{j=1}^{N}(x_j-\bar{x})^2 + \frac{n-1}{n}\frac{1}{N-1}\frac{1}{N}\sum_{i\neq j=1}^{N}(x_i-\bar{x})(x_j-\bar{x}) . \tag{35}$$

To evaluate the second sum in Eq (35) note that

$$\begin{aligned} 0 &= (N\bar{x}-N\bar{x})^2 = (x_1+\ldots+x_N-N\bar{x})^2 \\ &= (x_1-\bar{x}+\ldots+x_N-\bar{x})^2 \\ &= \sum_{j=1}^{N}(x_j-\bar{x})^2+\sum_{i\neq j=1}^{N}(x_i-\bar{x})(x_j-\bar{x}), \end{aligned} \tag{36}$$

giving

$$\sum_{i\neq j=1}^{N}(x_i-\bar{x})(x_j-\bar{x}) = -\sum_{j=1}^{N}(x_j-\bar{x})^2. \tag{37}$$

Finally, we have

$$s_n^2 = \left(\frac{1}{n} - \frac{n-1}{n}\frac{1}{N-1}\right)\frac{1}{N}\sum_{j=1}^{N}(x_j - \bar{x})^2 = \left(1 - \frac{n-1}{N-1}\right)\frac{1}{n}s_1^2 . \tag{38}$$

Eq (38) shows that in the limit of N large, the sample variance for subsets of size n is equal to the sample variance for single values divided by n, as one would expected. For finite N, however, there is a correction factor, less than one, which is equal to zero for $n = N$, as it should be. Using this correction factor will allow us to get a better estimate of the dependence of magnitude uncertainty on station coverage.

2.6. Magnitude Uncertainty (corrected)

For each event, i, we now correct the variance as computed in Eq (27), by using Eq (38) to adjust for each sample of size N_i used to compute $\bar{m}_i$. The corrected sample variance for subsets of size n in bin k is then

$$s^2_{n,\,k;\,\text{corrected}} = \frac{1}{N_{n,k}}\sum_{i=1}^{N_e}\left(\frac{N_i - 1}{N_i - n}\right)\sum_{\substack{1 \le j_1 < \ldots < j_n \le N_i \\ q_k < q < q_{k+1}}} e(j_1, \ldots, j_n)^2 . \tag{39}$$

Figure 7 is a plot of $s_{2,\,k;\,\text{corrected}}$ similar to Figure 4. Notice that the plot is basically shifted up by a small amount. In fact, the average square root of the variance of this curve times n (= 2) is 0.23, now equal to the single station value, s_s, given in Eq (13).

Figures 8, 9, and 10 plot $s_{n,\,k;\,\text{corrected}}$ for subsets with $n = 3, 4, 5$, respectively, and $A = 360°$, that is, no symmetry is assumed. For given n, only those events which have N_s greater than $n + 4$ are used, which reduces the number of events used as n increases. In each case, it can be seen that the general trend is for a decrease in Ms magnitude uncertainty as a function of increasing q. This is the expected result; the more the stations are evenly distributed around the unit circle, greater q, the less the expected variance in magnitude. The average variance for each case is approximately equal to the single station value divided by n, as expected from Eq (38). Note that the large error bars for the endpoints on some of the plots are due to the small number values which fall into the particular bin used to calculate the average. The seeming great decrease in uncertainty as a function of q for $n = 5$ should not be taken too seriously due to the large error bars on the endpoints.

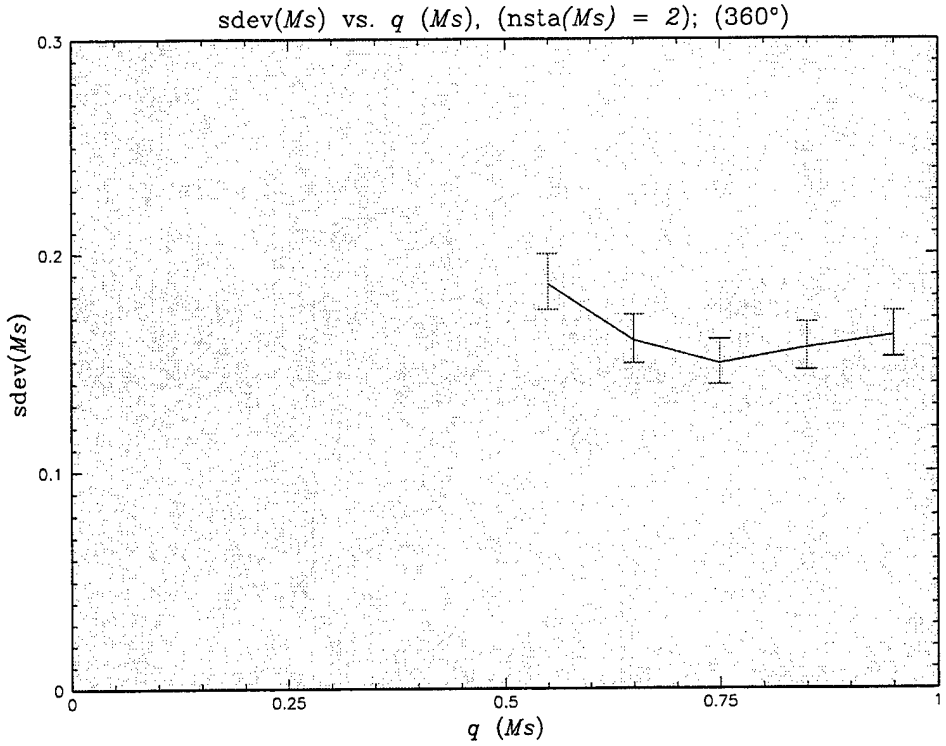

Figure 7. **Ms magnitude uncertainty versus station coverage for 2 station subsets, $A = 360°$ (corrected).**

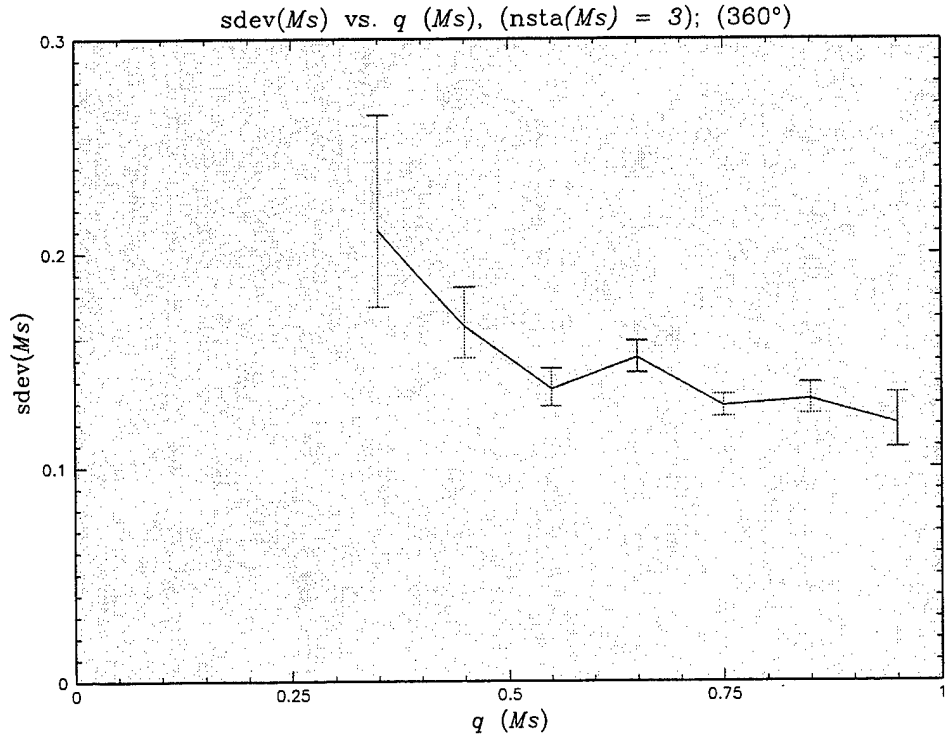

Figure 8. **Ms magnitude uncertainty versus station coverage for 3 station subsets, $A = 360°$ (corrected).**

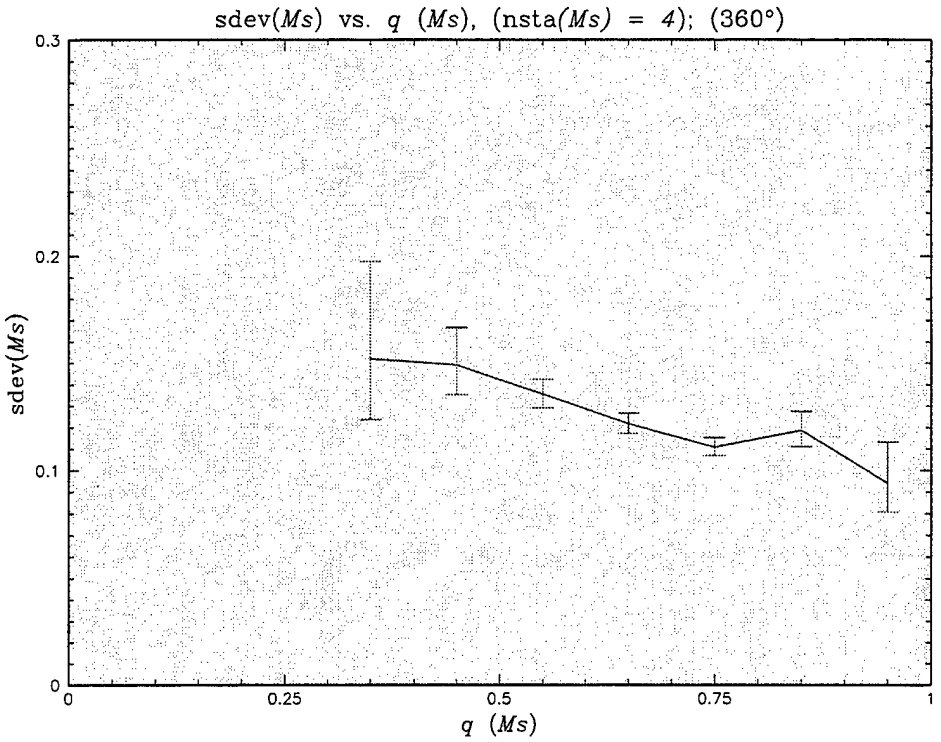

Figure 9. Ms magnitude uncertainty versus station coverage for 4 station subsets, A = 360° (corrected).

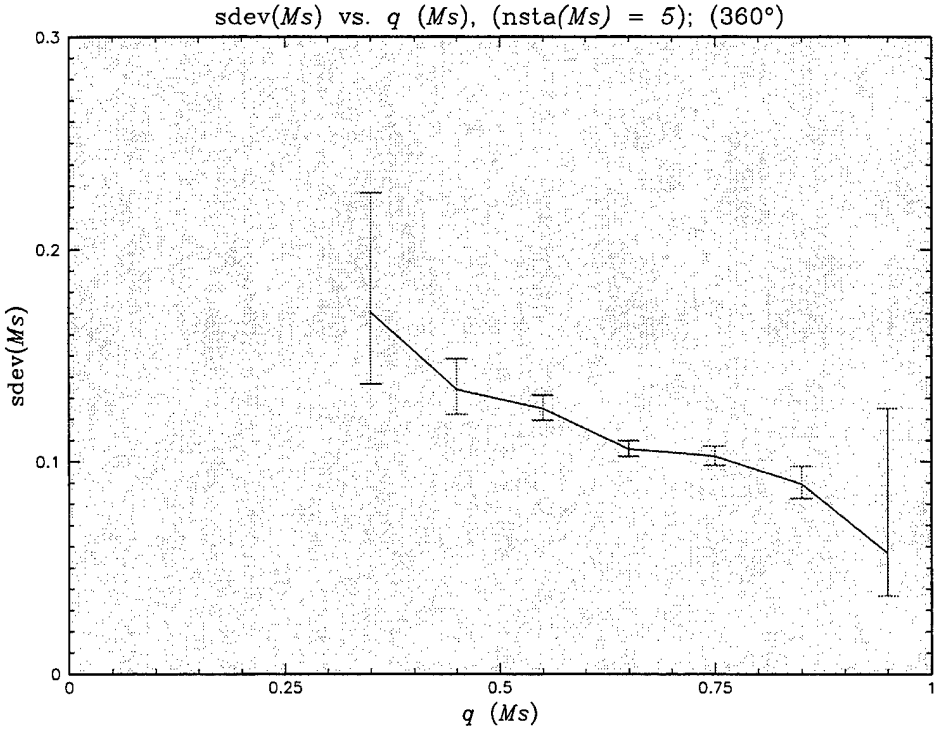

Figure 10. Ms magnitude uncertainty versus station coverage for 5 station subsets, A = 360° (corrected).

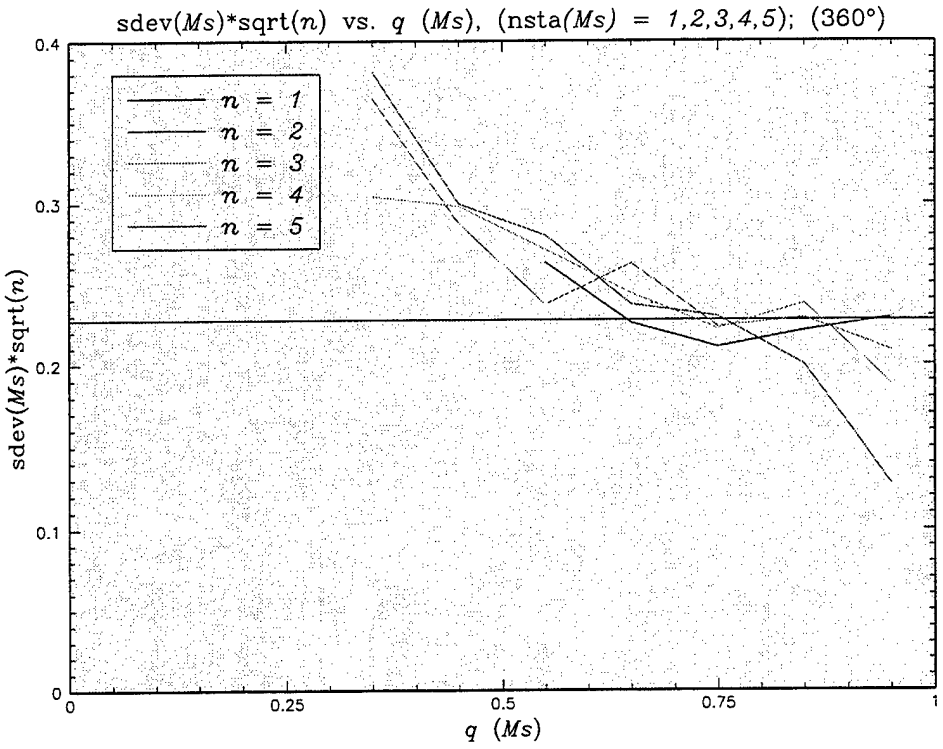

Figure 11. Ms magnitude uncertainty times the square root of number of stations versus station coverage for $n = 1, 2, 3.4, 5$, $A = 360°$ (corrected).

Figure 11 is a plot of $\sqrt{n} \times s_{n,\,k;\,\text{corrected}}$ as a function q for subsets with $n = 1, 2, 3, 4, 5$ and $A = 360°$, where the error bars have been suppressed for clarity. This plot combines each of the plots in Figures 7–10 times the square root of n. As expected, each of the curves has about the same average variance, approximately equal to $s_s = 0.23$, which is displayed as a horizontal line in the plot and labeled $n = 1$. Recalling that the endpoints were computed with very few data points and, therefore, have large error bars associated with them, the curves have approximately the same dependence on q, which implies that we have chosen a consistent definition of station coverage. In review, recall that these curves were computed by using Ms data from 400 events in the REB, which have been corrected for station bias. The bias was estimated from these events. The sample variance for subsets of a given size, n, were corrected for finite sample size, as in Eq (39), and each curve was then adjusted by multiplying by the square root of n. What remains should then be a good estimate of the true dependence of the Ms magnitude uncertainty on station coverage. If the definition of station coverage is chosen well, the station coverage dependence should be independent of n, as is approximately the case in Figure 11. In Figure 12 we combine Figures 7–10 for comparison, which have been off-set for clarity.

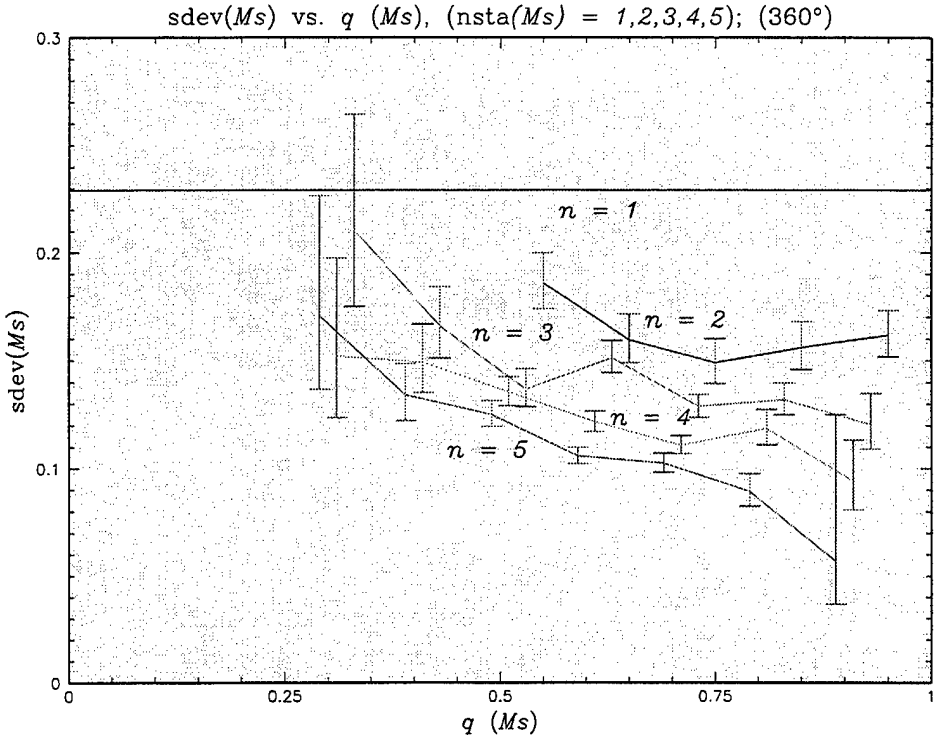

Figure 12. Ms magnitude uncertainty versus station coverage for n = 1, 2, 3.4, 5, A = 360° (corrected).

Figure 13 plots $s_{n,\,k;\,\text{corrected}}$ as a function of q for subsets with n = 1, 2, 3, 4, 5 and A = 180°, which assumes that the data is symmetric with respect to 180 degree rotations. It can be seen that for each n greater than one there is a general decrease in Ms magnitude uncertainty with increasing q, but that, compared to Figure 12, the slopes are not as steep. Although this is mild evidence that there is a 180 degree symmetry in the Ms data, it seems preferable not to make this assumption when attempting reduce Ms magnitude uncertainty when stations are well spread about the event location.

mb Magnitude Uncertainty

We now consider the relation between mb magnitude uncertainty and station coverage in an analogous manner as the Ms analysis described in detail above. Figures 14 and 15 are plots of $s_{n,\,k;\,\text{corrected}}$ for mb measurements as a function of q for subsets with n = 1, 2, 3, 4, 5 for A = 360° and A = 180°, respectively. Unlike the Ms case shown in Figure 12, the mb magnitude uncertainty for A = 360° does not show consistent decreasing trends as q increases, although there seems to be slight indications of decreasing trends when a 180 degree symmetry is assumed as shown in Figure 15.

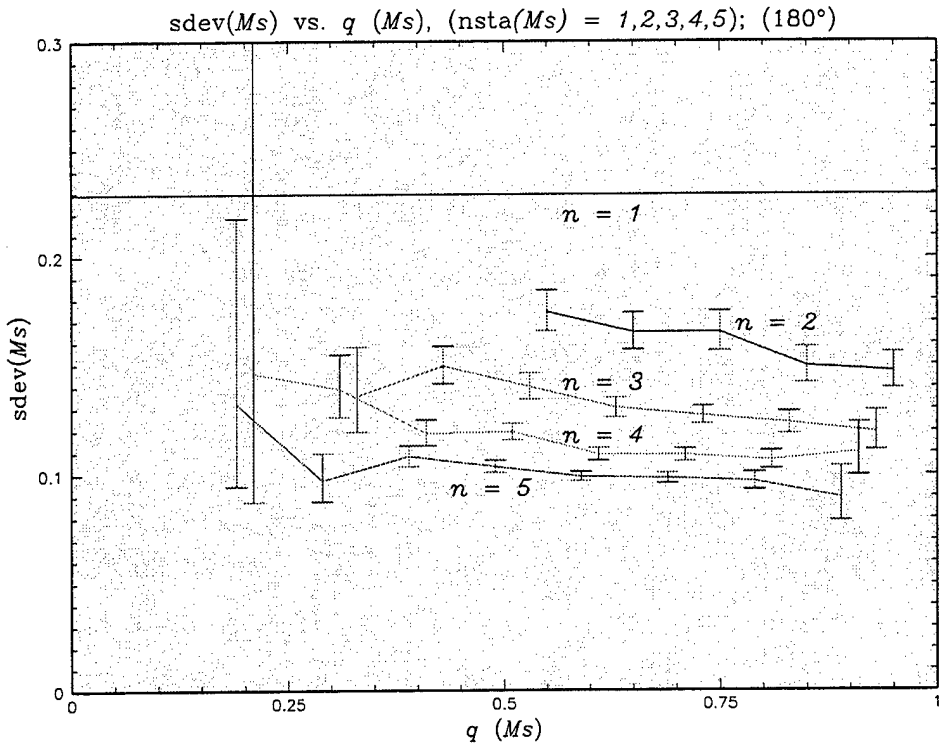

Figure 13. Ms magnitude uncertainty versus station coverage for n = 1, 2, 3.4, 5, A = 180° (corrected).

It should be noted that if the dependence on station coverage is due to the radiation pattern of the seismic wave, and this is not necessarily the case, then for mb magnitudes, which are produced by body waves, such a pattern would most readily be observed by mapping station locations to the focal sphere (see, for example, Aki and Richards, 1980). It is not clear that large q for mb measurements on the earth's surface correspond to large coverage of the focal sphere. To determine this, one would have to use raytracing techniques, which are beyond the scope of this study. The mild trends seen in the A = 180° case are not completely surprising, however, because any 180 degree symmetry in the radiation pattern on the focal sphere would approximately propagate to the surface due to the approximate spherical symmetry of the earth's interior. In any case, the dependence on q is small enough that for practical purposes we will say that there is no dependence of mb magnitude uncertainty on surface station coverage.

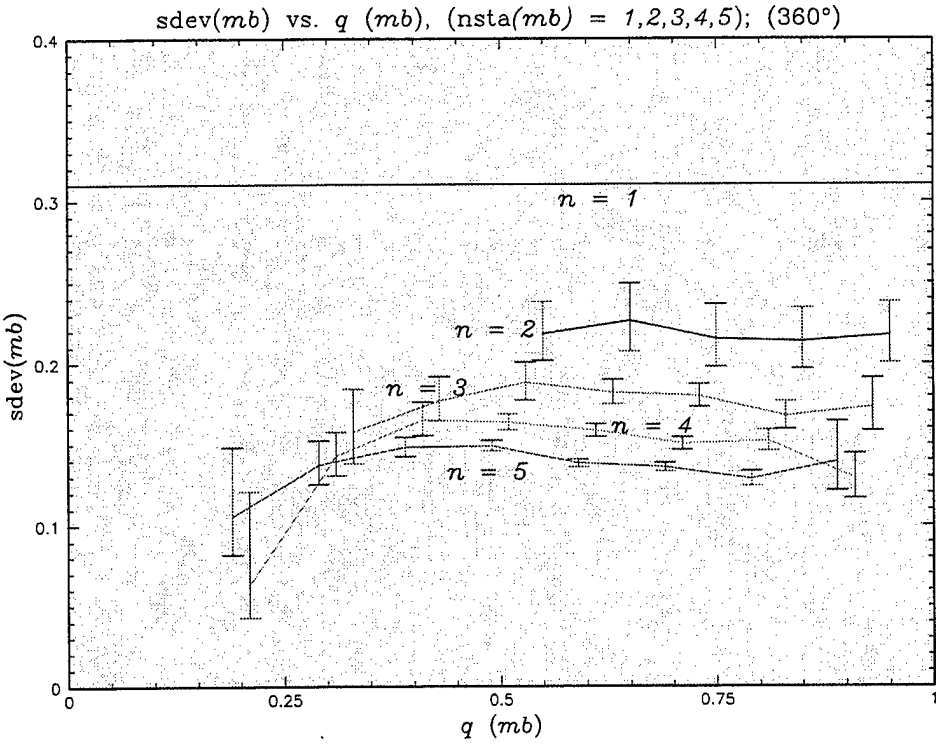

Figure 14. mb magnitude uncertainty versus station coverage for n = 1, 2, 3.4, 5 , A = 360° (corrected).

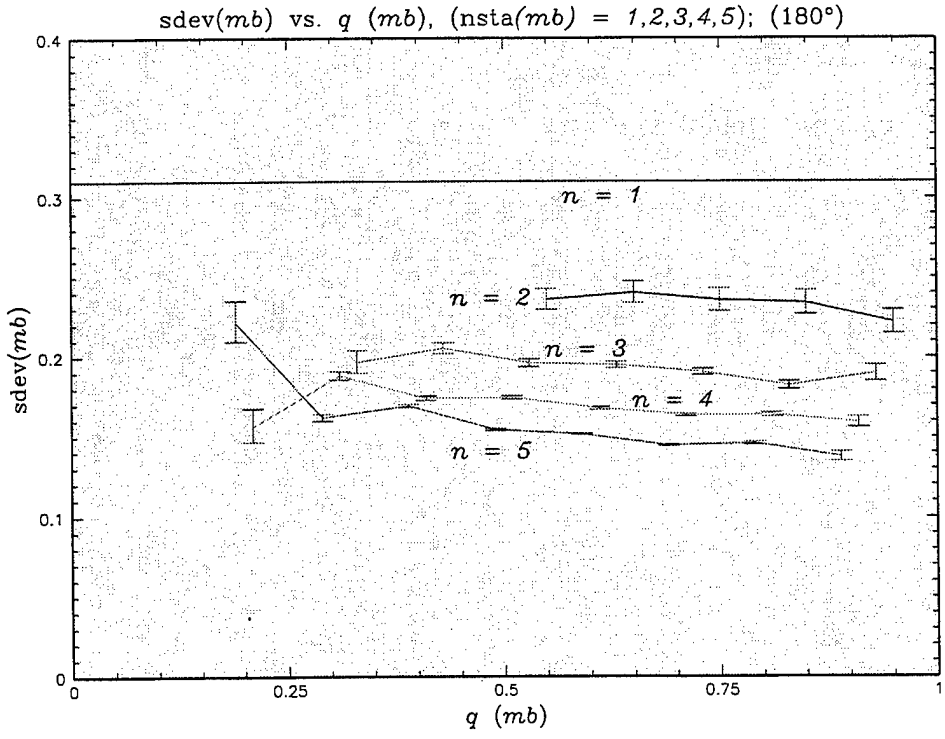

Figure 15. mb magnitude uncertainty versus station coverage for n = 1, 2, 3.4, 5 , A = 180° (corrected).

3. Multivariate Approach

In the previous section it was shown how the variance in Ms and mb measurements depends on station coverage. Generally speaking, as the stations observing Ms are more uniformly spread about the unit circle the smaller the variance. The dependence of the variance of mb measurements on station coverage is substantially less than for Ms measurements. Inspection of Figure 11, which plots (corrected) Ms magnitude uncertainty (standard deviation) times the square root of n, the number of stations, as function of q, the station coverage, for n equal to 1, 2, 3, 4, and 5, shows that the dependence of the Ms uncertainty on q, once scaled by the square root of n, is essentially independent of n. This suggests that the portion of the variance of the mean of Ms for a given set of n measurements, which depends on station coverage, can be determined by the relative correlation between each pair of stations, as a function only of the angle made by the two stations with respect to the event location. Whether this assumption is warranted or not for the actual REB data will be addressed below. A multivariate approach is most suited in this case.

3.1. Uncertainty in mb–Ms Using Multivariate Statistical Analysis

We wish to generalize the expression for the variance of $\overline{m}_b - \overline{M}_s$ given in Eq (5) by considering the correlations between stations for Ms measurements as a function of station angle. We will assume that there is no correlation in the individual mb measurements, as discussed above, and that there is no correlation between Ms and mb measurements. In fact, for the 400 events we are considering in the REB, the sample correlation coefficient between Ms and mb measurements, using those station measurements that have both Ms and mb readings, is approximately 0.06, so this assumption is well justified. Under these assumptions, the variance of $\overline{m}_b - \overline{M}_s$, denoted by σ^2, is given by

$$\sigma^2 = \text{variance}(\overline{m}_b - \overline{M}_s) = \frac{\sigma_b^2}{N_b} + \text{variance}(\overline{M}_s). \tag{40}$$

To calculate the variance of $\overline{M}_s$, suppose that for a given event there are n Ms measurements assumed to be given by the n components of a random vector $\mathbf{x} = (x_1, \ldots, x_n)'$, such that

$$x_j = m + e_j, \qquad j = 1, \ldots, n, \tag{41}$$

where m is the mean of each measurement, assumed to be the same for all $j = 1, \ldots, n$, and $E(e_j e_k) = \Sigma_{jk}$. In vector notation we have

$$\mathbf{x} = m\mathbf{a} + \mathbf{e}, \qquad E(\mathbf{e}\mathbf{e}') = \Sigma, \tag{42}$$

where $\mathbf{a}$ is a vector with all components equal to one, $\mathbf{a} = (1, \ldots, 1)'$. Any linear combination of the x_j of the form

$$z = \mathbf{c}'\mathbf{x}, \qquad \text{with} \quad \mathbf{c}'\mathbf{a} = 1, \tag{43}$$

has mean equal to m, $E(z) = m$, and variance equal to $\mathbf{c}'\Sigma\mathbf{c}$. In particular, if $\mathbf{c} = (1/n)\mathbf{a}$, then z is equal to the usual sample mean, $\overline{M}_s$, with variance

$$\text{variance}(\overline{M}_s) = \frac{1}{N_s^2}\mathbf{a}'\Sigma\mathbf{a}, \tag{44}$$

where we have now written N_s for n.

We also note for reference that if $\mathbf{c} = (\mathbf{a}'\Sigma^{-1}\mathbf{a})^{-1}\Sigma^{-1}\mathbf{a}$, then z, under the assumption of normality, gives the maximum likelihood estimate (MLE) of m, which is also the linear combination having mean m with minimum variance, equal to $(\mathbf{a}'\Sigma^{-1}\mathbf{a})^{-1}$.

We now assume that for a given event, the covariance matrix, Σ, has the form

$$\Sigma_{jj} = \sigma_s^2, \qquad j = 1, \ldots, N_s, \tag{45}$$

$$\Sigma_{jk} = \rho_{jk}\sigma_s^2, \qquad j \neq k = 1, \ldots, N_s, \tag{46}$$

where

$$\rho_{jk} = f(\cos(\alpha_k - \alpha_j)), \tag{47}$$

and α_j is the azimuthal angle of station j relative to the event location. That is, the variance of each Ms measurement at each station is assumed to be the same, whose value is given in Eq (10) when corrections for station bias are not used or Eq (13) if corrected for bias, and the correlation coefficient, ρ_{jk}, depends only on the angular separation of station j and k with respect to the event location. The function f will be estimated from the REB data in the next section.

3.2. The Correlation Coefficient

To estimate the function f in Eq (47) we can use the curve plotted in Figure 7 for Ms magnitude standard deviation as a function of q for two station subsets. From the definition of q for two stations it is readily seen that $\alpha = 2\pi(q - 1/2)$, where α is the angle made by the two stations with respect to the event location. To convert the variances in Figure 7 to correlation coefficients note that for the random variable $(x + y)/2$,

$$\sigma^2_{(x+y)/2} = \sigma^2_{x/2} + \sigma^2_{y/2} + 2\mathrm{cov}\left(\frac{x}{2}, \frac{y}{2}\right) = \frac{1}{4}\sigma^2_x + \frac{1}{4}\sigma^2_y + \frac{1}{2}\mathrm{cov}(x, y). \tag{48}$$

Assuming that $\sigma^2_x = \sigma^2_y = \sigma^2_s$, we have

$$\rho = \frac{\mathrm{cov}(x, y)}{\sigma_x \sigma_y} = 2\frac{\sigma^2_{(x+y)/2}}{\sigma^2_s} - 1. \tag{49}$$

Using this transformation we plot in Figure 16 the correlation coefficient as a function of cosine of the angle between two stations for all two station subsets in the REB database with total number of Ms measurements greater than six. The data has been split into five bins.

To select the function f, we fit the five points in Figure 16 with a function of the form

$$f(\cos\alpha) = b_0 + b_1\cos\alpha + b_2\cos^2\alpha. \tag{50}$$

Using least squares the coefficients are

$$b_0 = -0.17, \quad b_1 = 0.13, \quad b_2 = 0.35. \tag{51}$$

The function $f(\cos\alpha)$ is also plotted (the smooth curve) in Figure 16. Notice that for small station angles, cosine near one, the correlation is positive, suggesting that stations which have angles from an event which are close have Ms measurements that tend to be above average or below average. For station angles close to 90 degrees, cosine near zero, the correlation coefficient is negative, consistent with radiation patterns that are larger than average in a given direction and smaller than average in a direction 90 degrees from the first direction. The correlation coefficient for stations diametrically opposed, cosine near minus one, is nearly zero. If the effect of radiation patterns with 180 degree rotational symmetry were strong, we would expect this value to be

positive, the same as zero degrees. Since this is not the case, we will make no assumptions about the symmetry properties of the correlation coefficient function.

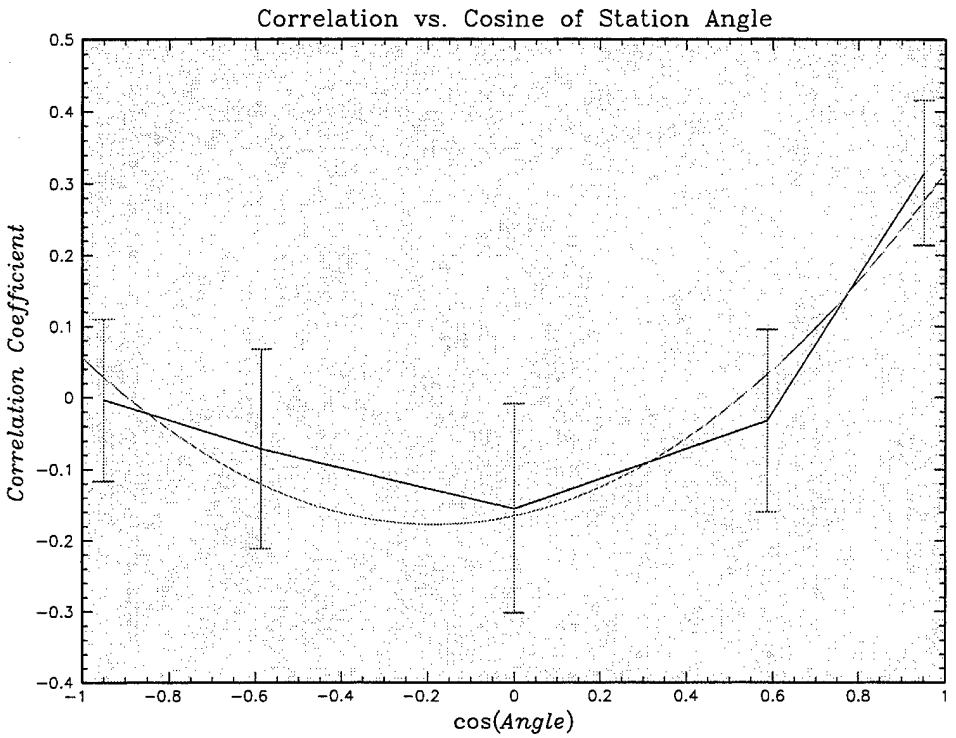

Figure 16. Correlation coefficient as a function of cosine of the station angle for 2 station subsets and smooth fit.

3.3. The Consistency of the Correlation Coefficient Function

It will be recalled that we have assumed that the correlation of two Ms magnitude measurements for a single event is independent of event location and depends only on the angle the two stations make with the event location. If this were not true, then it would be possible for the function given in Eq (50), which was estimated using actual data, to give inconsistent results, that is, it would be possible for the covariance matrix, Σ, defined by Eq (45) and (46) to not be positive definite, which it must be if it were a true covariance matrix. If we can prove that Σ is always positive definite for all choices of station angles, then our correlation function is consistent, although, of course, it does not prove that the assumption that the correlation depends only on station angle is true. We will prove below the somewhat weaker result, although it may be equivalent, that the variance of $\overline{M}_s$, as given in Eq (44), is always positive.

Using $\mathbf{a} = (1, \ldots, 1)'$ Eq (44) gives

$$\text{variance}(\overline{M}_s) = \frac{1}{N_s^2}\mathbf{a}'\Sigma\mathbf{a} = \frac{\sigma_s^2}{N_s}\left[1 + \frac{2}{N_s}\left(\sum_{1 \le j < k \le N_s} \rho_{jk}\right)\right]. \tag{52}$$

Defining

$$F(\alpha_1, \ldots, \alpha_n) = \sum_{1 \le j < k \le n} \rho_{jk} = \sum_{1 \le j < k \le n} f(\cos(\alpha_k - \alpha_j)), \tag{53}$$

we must show that $F(\alpha_1, \ldots, \alpha_n) > -n/2$ for all α_j, $j = 1, \ldots, n$ and all n.

We first show that if $f(x)$ is convex for $-1 \le x \le 1$, that is,

$$f(\lambda x + (1-\lambda)y) \le \lambda f(x) + (1-\lambda)f(y), \tag{54}$$

whenever $-1 \le x < y \le 1$ and $0 \le \lambda \le 1$, then F achieves its minimum when the α_j are evenly spaced. For functions with continuous second derivatives, convexity is equivalent to having $f''(x) \ge 0$ for $-1 \le x \le 1$. Since, as is easily shown, $F(\alpha_1 + \alpha, \ldots, \alpha_n + \alpha) = F(\alpha_1, \ldots, \alpha_n)$ for all α, it is sufficient to show that $F(0, 2\pi/n, \ldots, (n-1)2\pi/n) \le F(\alpha_1, \ldots, \alpha_n)$ for all α_j. To see this, notice that if some α_j, say α_1, was not equal to 0 then half of the terms in Eq (53) which contain α_1 will have arguments of f which increase, by Δx, say, and the other half will have arguments that decrease by Δx, because the points are evenly spaced on the unit circle (if n is even the point that is diametrically opposed can be written $f = f/2 + f/2$ and the argument is the same). By the convex property of f with $\lambda = 1/2$,

$$f(x - \Delta x) + f(x + \Delta x) \ge 2f(x), \tag{55}$$

which shows

$$F(0, \ldots, (j+1)2\pi/n, \ldots, (n-1)2\pi/n) \le F(0, \ldots, (j+1)2\pi/n + \alpha, \ldots, (n-1)2\pi/n) \tag{56}$$

for all α. The extension to two variables at a time and finally to all n variables is similar but tedious. For example, for two variables, inequalities such as

$$f(x+\Delta x_1)+f(x-\Delta x_1+\Delta x_2)+f(x-\Delta x_2)\geq 2f(x+\Delta x_2/2)+f(x-\Delta x_2) \qquad (57)$$
$$\geq 2f(x+\Delta x_2/2)+2f(x-\Delta x_2/2)-f(x)\geq 3f(x),$$

must be employed.

Having shown that F achieves its minimum when the α_j are evenly spaced, we must have

$$F(0, 2\pi/n, \ldots, n-12\pi/n) = \sum_{j=1}^{n-1}(n-j)f\left(\cos\left(j\frac{2\pi}{n}\right)\right) > -\frac{n}{2}. \qquad (58)$$

That is, the convex function, f, must satisfy

$$\sum_{j=1}^{\frac{n}{2}-1} f\left(\cos\left(j\frac{2\pi}{n}\right)\right)+\frac{1}{2}f(-1) > -\frac{1}{2}, \qquad \text{for } n \text{ even}, \qquad (59)$$

and

$$\sum_{j=1}^{\frac{n-1}{2}} f\left(\cos\left(j\frac{2\pi}{n}\right)\right) > -\frac{1}{2}, \qquad \text{for } n \text{ odd}. \qquad (60)$$

Note, these equations show that f can not be entirely negative, i.e., Ms measurements can not be negatively correlated for all angles.

It now remains to show for f given in Eq (50) and (51), which is clearly convex, Eq (59) and (60) are satisfied for all n. Figure 17 plots the left hand sides of Eq (59) (for n even) and Eq (60) (for n odd) for $n = 1, \ldots, 30$. It is apparent that sums are well above –1/2 for all n. To show this for large n, denote the left hand side of Eq (60) by s_n. Then

$$s_n \sim \sum_{j=1}^{n/2} b_0 + b_1\cos\left(j\frac{2\pi}{n}\right)+b_2\cos^2\left(j\frac{2\pi}{n}\right). \qquad (61)$$

For large n,

$$\sum_{j=1}^{n/2}\cos^2\left(j\frac{2\pi}{n}\right)\frac{2\pi}{n} \sim \int_0^{\pi}\cos^2 x\,dx = \frac{\pi}{2}, \qquad (62)$$

and

$$\sum_{j=1}^{n/2} \cos\left(j\frac{2\pi}{n}\right) \sim 0, \tag{63}$$

giving

$$s_n \sim \frac{n}{2}\left(b_0 + \frac{b_2}{2}\right) \sim 0.003n, \tag{64}$$

which is positive and, therefore, greater than –1/2. We have now shown that for all N_s, all α_j, $j = 1, \ldots, N_s$, and f chosen as in Eq (50) and (51), the variance of $\overline{M}_s$ is always positive.

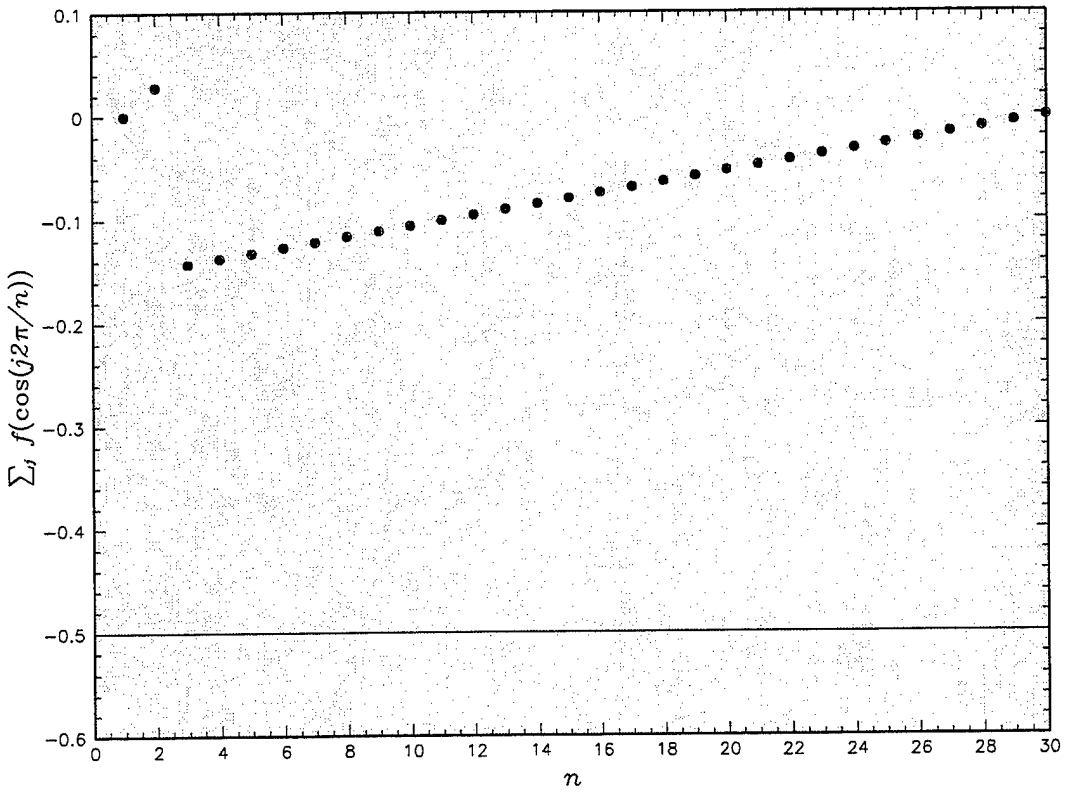

Figure 17. Left hand side of Eq (59) for *n* even and Eq (60) for *n* odd versus *n*.

3.4. Results

We now apply our formula for the variance of $\overline{m}_b - \overline{M}_s$, given in Eq (40) and using Eq (44)–(47), (50) and (51), to all 400 events in the REB database with the number of Ms measurements greater than six. For each event we calculate the variance of $\overline{M}_s$ as in Eq (44) and the variance of $\overline{m}_b - \overline{M}_s$ as in Eq (40). The square root of the average variance of $\overline{M}_s$ times N_s over the 400 events was 0.34. If there had been no correlation between stations, this value would have been 0.28, the unbiased sample standard deviation. We can see that the value with correlation is larger, indicating that on average, the events in the data base have positive correlation. The square root of the average variance of $\overline{m}_b$ times N_b plus the average variance of $\overline{M}_s$ times N_s over the 400 events was 0.52, compared to 0.48 if there had been no correlation. Thus, on average the effect of correlation is small, but can vary for different events, depending on the azimuthal coverage of the stations which recorded them. If $N_s = 4$, for example, the minimum value of $\sqrt{N_s \mathrm{var}(\overline{M}_s)}$ is $0.84 \cdot \sigma_s$ and the maximum value is $1.39 \cdot \sigma_s$, a range in values of 55%.

4. Conclusions and Recommendations

Until the magnitude panel has provided its conclusions on magnitude estimates and their uncertainties, we recommend using the following formulas to estimate the uncertainty in mb–Ms. The variance of $\overline{m}_b - \overline{M}_s$, denoted by σ^2, is given by

$$\sigma^2 = \frac{\sigma_b^2}{N_b} + \text{variance}(\overline{M}_s), \tag{65}$$

where

$$\text{variance}(\overline{M}_s) = \frac{\sigma_s^2}{N_s}\left[1 + \frac{2}{N_s}\left(\sum_{1 \le j < k \le N_s} f(\cos(\alpha_k - \alpha_j))\right)\right], \tag{66}$$

$$f(\cos\alpha) = -0.17 + 0.13\cos\alpha + 0.35\cos^2\alpha. \tag{67}$$

Here, N_b is the number of mb measurements, N_s is the number of Ms (station) measurements, and α_j, $j = 1, \ldots, N_s$, is the azimuthal angle with respect to the event location of Ms measurement j. If station measurements are not corrected for bias, we recommend

$$\sigma_b = 0.39, \qquad \sigma_s = 0.28. \tag{68}$$

If each station measurement is corrected by the average bias for current data in the REB, we estimate the corrections will give

$$\sigma_b = 0.34, \qquad \sigma_s = 0.25. \tag{69}$$

We anticipate that these values will be improved by the magnitude panel with all appropriate systematic errors removed.

Finally, an event with measured $\overline{m}_b - \overline{M}_s$ is screened at the $100(1-\alpha)\%$ confidence level if

$$\overline{m}_b - \overline{M}_s + x_\alpha \sigma < 1.2, \tag{70}$$

where x_α is defined such that $\text{Prob}(x > x_\alpha) = \alpha$ for x distributed as normal with zero mean and unit variance.

5. References

Aki, K. and P. G. Richards (1980). *Quantitative Seismology*, W. H. Freeman and Company, New York.

Blandford, R. R., A. Dainty, R. Lacoss, R. Maxion, A. Ryall, B. Stump, C. Thurber, and T. Wallace (1992). Report on the DARPA Seismic Identification Workshop, Center for Seismic Studies, Arlington, VA, 18-19 May 1992.

Fisk, M. D., H. L. Gray and G. D. McCartor (1995). Statistical Methodology and Assessment of Seismic Event Characterization Capability, PL-TR-95-2156, Phillips Laboratory, Hanscom AFB, MA, ADA305487.

Israelsson, H. (1996). Private Communication.

Jepsen, D. (1996). Private Communication.

Marshall, P. D. and P. W. Basham (1972). Discrimination between earthquakes and underground explosions employing an improved Ms scale, *Geophys. J. R. Astro. Soc.*, **28**, 431–458.

McLaughlin, K. L., (1996). Private Communication.

McLaughlin, K. L., R. H. Shumway and T. W. McElfresh (1988). Determination of event magnitudes with correlated data and censoring: A maximum likelihood approach, *Geophysical Journal*, **95**, pages 31–44.

Rautian, T. G. and V. I. Khalturin (1994). The Multi-Factor Model of Magnitude Residuals and the Problem of the Precise Determination of Magnitude, PL-TR-94-2291, Phillips Laboratory, Hanscom AFB, MA, ADA310736.

von Seggern, D. (1970). The Effects of Radiation Patterns on Magnitudes Estimates, *Bulletin of the Seismological Society of America*, **60**, No. 2, pages 503–516.

THOMAS AHRENS
SEISMOLOGICAL LABORATORY 252-21
CALIFORNIA INSTITUTE OF TECHNOLOGY
PASADENA, CA 91125

RALPH ALEWINE
NTPO
1901 N. MOORE STREET, SUITE 609
ARLINGTON, VA 22209

SHELTON ALEXANDER
PENNSYLVANIA STATE UNIVERSITY
DEPARTMENT OF GEOSCIENCES
537 DEIKE BUILDING
UNIVERSITY PARK, PA 16801

MUAWIA BARAZANGI
INSTITUTE FOR THE STUDY OF THE CONTINENTS
3126 SNEE HALL
CORNELL UNIVERSITY
ITHACA, NY 14853

RICHARD BARDZELL
ACIS
DCI/ACIS
WASHINGTON, DC 20505

T.G. BARKER
MAXWELL TECHNOLOGIES
P.O. BOX 23558
SAN DIEGO, CA 92123

DOUGLAS BAUMGARDT
ENSCO INC.
5400 PORT ROYAL ROAD
SPRINGFIELD, VA 22151

THERON J. BENNETT
MAXWELL TECHNOLOGIES
11800 SUNRISE VALLEY DRIVE SUITE 1212
RESTON, VA 22091

WILLIAM BENSON
NAS/COS
ROOM HA372
2001 WISCONSIN AVE. NW
WASHINGTON, DC 20007

JONATHAN BERGER
UNIVERSITY OF CA, SAN DIEGO
SCRIPPS INSTITUTION OF OCEANOGRAPHY IGPP, 0225
9500 GILMAN DRIVE
LA JOLLA, CA 92093-0225

ROBERT BLANDFORD
AFTAC
1300 N. 17TH STREET
SUITE 1450
ARLINGTON, VA 22209-2308

STEVEN BRATT
NTPO
1901 N. MOORE STREET, SUITE 609
ARLINGTON, VA 22209

RHETT BUTLER
IRIS
1616 N. FORT MEYER DRIVE
SUITE 1050
ARLINGTON, VA 22209

LESLIE A. CASEY
DOE
1000 INDEPENDENCE AVE. SW
NN-40
WASHINGTON, DC 20585-0420

CATHERINE DE GROOT-HEDLIN
SCRIPPS INSTITUTION OF OCEANOGRAPHY
UNIVERSITY OF CALIFORNIA, SAN DIEGO
INSTITUTE OF GEOPHYSICS AND PLANETARY PHYSICS
LA JOLLA, CA 92093

STANLEY DICKINSON
AFOSR
110 DUNCAN AVENUE, SUITE B115
BOLLING AFB
WASHINGTON, D.C. 20332-001

SEAN DORAN
ACIS
DCI/ACIS
WASHINGTON , DC 20505

DIANE I. DOSER
DEPARTMENT OF GEOLOGICAL SCIENCES
THE UNIVERSITY OF TEXAS AT EL PASO
EL PASO, TX 79968

RICHARD J. FANTEL
BUREAU OF MINES
DEPT OF INTERIOR, BLDG 20
DENVER FEDERAL CENTER
DENVER, CO 80225

JOHN FILSON
ACIS/TMG/NTT
ROOM 6T11 NHB
WASHINGTON, DC 20505

MARK D. FISK
MISSION RESEARCH CORPORATION
735 STATE STREET
P.O. DRAWER 719
SANTA BARBARA, CA 93102-0719

LORI GRANT
MULTIMAX, INC.
311C FOREST AVE. SUITE 3
PACIFIC GROVE, CA 93950

I. N. GUPTA
MULTIMAX, INC.
1441 MCCORMICK DRIVE
LARGO, MD 20774

JAMES HAYES
NSF
4201 WILSON BLVD., ROOM 785
ARLINGTON, VA 22230

MICHAEL HEDLIN
UNIVERSITY OF CALIFORNIA, SAN DIEGO
SCRIPPS INSTITUTION OF OCEANOGRAPHY IGPP, 0225
9500 GILMAN DRIVE
LA JOLLA, CA 92093-0225

EUGENE HERRIN
SOUTHERN METHODIST UNIVERSITY
DEPARTMENT OF GEOLOGICAL SCIENCES
DALLAS, TX 75275-0395

VINDELL HSU
HQ/AFTAC/TTR
1030 S. HIGHWAY A1A
PATRICK AFB, FL 32925-3002

RONG-SONG JIH
PHILLIPS LABORATORY
EARTH SCIENCES DIVISION
29 RANDOLPH ROAD
HANSCOM AFB, MA 01731-3010

LAWRENCE LIVERMORE NATIONAL LABORATORY
ATTN: TECHNICAL STAFF (PLS ROUTE)
PO BOX 808, MS L-200
LIVERMORE, CA 94551

LAWRENCE LIVERMORE NATIONAL LABORATORY
ATTN: TECHNICAL STAFF (PLS ROUTE)
PO BOX 808, MS L-221
LIVERMORE, CA 94551

ROBERT GEIL
DOE
PALAIS DES NATIONS, RM D615
GENEVA 10, SWITZERLAND

HENRY GRAY
SMU STATISTICS DEPARTMENT
P.O. BOX 750302
DALLAS, TX 75275-0302

DAVID HARKRIDER
PHILLIPS LABORATORY
EARTH SCIENCES DIVISION
29 RANDOLPH ROAD
HANSCOM AFB, MA 01731-3010

THOMAS HEARN
NEW MEXICO STATE UNIVERSITY
DEPARTMENT OF PHYSICS
LAS CRUCES, NM 88003

DONALD HELMBERGER
CALIFORNIA INSTITUTE OF TECHNOLOGY
DIVISION OF GEOLOGICAL & PLANETARY SCIENCES
SEISMOLOGICAL LABORATORY
PASADENA, CA 91125

ROBERT HERRMANN
ST. LOUIS UNIVERSITY
DEPARTMENT OF EARTH & ATMOSPHERIC SCIENCES
3507 LACLEDE AVENUE
ST. LOUIS, MO 63103

ANTHONY IANNACCHIONE
BUREAU OF MINES
COCHRANE MILL ROAD
PO BOX 18070
PITTSBURGH, PA 15236-9986

THOMAS JORDAN
MASSACHUSETTS INSTITUTE OF TECHNOLOGY
EARTH, ATMOSPHERIC & PLANETARY SCIENCES
77 MASSACHUSETTS AVENUE, 54-918
CAMBRIDGE, MA 02139

LAWRENCE LIVERMORE NATIONAL LABORATORY
ATTN: TECHNICAL STAFF (PLS ROUTE)
PO BOX 808, MS L-207
LIVERMORE, CA 94551

LAWRENCE LIVERMORE NATIONAL LABORATORY
ATTN: TECHNICAL STAFF (PLS ROUTE)
LLNL
PO BOX 808, MS L-175
LIVERMORE, CA 94551

LAWRENCE LIVERMORE NATIONAL LABORATORY
ATTN: TECHNICAL STAFF (PLS ROUTE)
PO BOX 808, MS L-208
LIVERMORE, CA 94551

LAWRENCE LIVERMORE NATIONAL LABORATORY
ATTN: TECHNICAL STAFF (PLS ROUTE)
PO BOX 808, MS L-202
LIVERMORE, CA 94551

LAWRENCE LIVERMORE NATIONAL LABORATORY
ATTN: TECHNICAL STAFF (PLS ROUTE)
PO BOX 808, MS L-195
LIVERMORE, CA 94551

LAWRENCE LIVERMORE NATIONAL LABORATORY
ATTN: TECHNICAL STAFF (PLS ROUTE)
PO BOX 808, MS L-205
LIVERMORE, CA 94551

THORNE LAY
UNIVERSITY OF CALIFORNIA, SANTA CRUZ
EARTH SCIENCES DEPARTMENT
EARTH & MARINE SCIENCE BUILDING
SANTA CRUZ, CA 95064

ANATOLI L. LEVSHIN
DEPARTMENT OF PHYSICS
UNIVERSITY OF COLORADO
CAMPUS BOX 390
BOULDER, CO 80309-0309

DONALD A. LINGER
DNA
6801 TELEGRAPH ROAD
ALEXANDRIA, VA 22310

LOS ALAMOS NATIONAL LABORATORY
ATTN: TECHNICAL STAFF (PLS ROUTE)
PO BOX 1663, MS F659
LOS ALAMOS, NM 87545

LOS ALAMOS NATIONAL LABORATORY
ATTN: TECHNICAL STAFF (PLS ROUTE)
PO BOX 1663, MS F665
LOS ALAMOS, NM 87545

LOS ALAMOS NATIONAL LABORATORY
ATTN: TECHNICAL STAFF (PLS ROUTE)
PO BOX 1663, MS D460
LOS ALAMOS, NM 87545

LOS ALAMOS NATIONAL LABORATORY
ATTN: TECHNICAL STAFF (PLS ROUTE)
PO BOX 1663, MS C335
LOS ALAMOS, NM 87545

GARY MCCARTOR
SOUTHERN METHODIST UNIVERSITY
DEPARTMENT OF PHYSICS
DALLAS, TX 75275-0395

KEITH MCLAUGHLIN
MAXWELL TECHNOLOGIES
P.O. BOX 23558
SAN DIEGO, CA 92123

BRIAN MITCHELL
DEPARTMENT OF EARTH & ATMOSPHERIC SCIENCES
ST. LOUIS UNIVERSITY
3507 LACLEDE AVENUE
ST. LOUIS, MO 63103

RICHARD MORROW
USACDA/IVI
320 21ST STREET, N.W.
WASHINGTON, DC 20451

JOHN MURPHY
MAXWELL TECHNOLOGIES
11800 SUNRISE VALLEY DRIVE SUITE 1212
RESTON, VA 22091

JAMES NI
NEW MEXICO STATE UNIVERSITY
DEPARTMENT OF PHYSICS
LAS CRUCES, NM 88003

JOHN ORCUTT
INSTITUTE OF GEOPHYSICS AND PLANETARY PHYSICS
UNIVERSITY OF CALIFORNIA, SAN DIEGO
LA JOLLA, CA 92093

PACIFIC NORTHWEST NATIONAL LABORATORY
ATTN: TECHNICAL STAFF (PLS ROUTE)
PO BOX 999, MS K6-48
RICHLAND, WA 99352

PACIFIC NORTHWEST NATIONAL LABORATORY
ATTN: TECHNICAL STAFF (PLS ROUTE)
PO BOX 999, MS K7-34
RICHLAND, WA 99352

PACIFIC NORTHWEST NATIONAL LABORATORY
ATTN: TECHNICAL STAFF (PLS ROUTE)
PO BOX 999, MS K6-40
RICHLAND, WA 99352

PACIFIC NORTHWEST NATIONAL LABORATORY
ATTN: TECHNICAL STAFF (PLS ROUTE)
PO BOX 999, MS K5-72
RICHLAND, WA 99352

PACIFIC NORTHWEST NATIONAL LABORATORY
ATTN: TECHNICAL STAFF (PLS ROUTE)
PO BOX 999, MS K5-12
RICHLAND, WA 99352

KEITH PRIESTLEY
DEPARTMENT OF EARTH SCIENCES
UNIVERSITY OF CAMBRIDGE
MADINGLEY RISE, MADINGLEY ROAD
CAMBRIDGE, CB3 OEZ UK

PAUL RICHARDS
COLUMBIA UNIVERSITY
LAMONT-DOHERTY EARTH OBSERVATORY
PALISADES, NY 10964

CHANDAN SAIKIA
WOOODWARD-CLYDE FEDERAL SERVICES
566 EL DORADO ST., SUITE 100
PASADENA, CA 91101-2560

SANDIA NATIONAL LABORATORY
ATTN: TECHNICAL STAFF (PLS ROUTE)
DEPT. 6116
MS 0750, PO BOX 5800
ALBUQUERQUE, NM 87185-0750

SANDIA NATIONAL LABORATORY
ATTN: TECHNICAL STAFF (PLS ROUTE)
DEPT. 9311
MS 1159, PO BOX 5800
ALBUQUERQUE, NM 87185-1159

SANDIA NATIONAL LABORATORY
ATTN: TECHNICAL STAFF (PLS ROUTE)
DEPT. 5736
MS 0655, PO BOX 5800
ALBUQUERQUE, NM 87185-0655

THOMAS SERENO JR.
SCIENCE APPLICATIONS INTERNATIONAL
CORPORATION
10260 CAMPUS POINT DRIVE
SAN DIEGO, CA 92121

PACIFIC NORTHWEST NATIONAL LABORATORY
ATTN: TECHNICAL STAFF (PLS ROUTE)
PO BOX 999, MS K7-22
RICHLAND, WA 99352

PACIFIC NORTHWEST NATIONAL LABORATORY
ATTN: TECHNICAL STAFF (PLS ROUTE)
PO BOX 999, MS K6-84
RICHLAND, WA 99352

FRANK PILOTTE
HQ/AFTAC/TT
1030 S. HIGHWAY A1A
PATRICK AFB, FL 32925-3002

JAY PULLI
RADIX SYSTEMS, INC.
6 TAFT COURT
ROCKVILLE, MD 20850

DAVID RUSSELL
HQ AFTAC/TTR
1030 SOUTH HIGHWAY A1A
PATRICK AFB, FL 32925-3002

SANDIA NATIONAL LABORATORY
ATTN: TECHNICAL STAFF (PLS ROUTE)
DEPT. 5704
MS 0979, PO BOX 5800
ALBUQUERQUE, NM 87185-0979

SANDIA NATIONAL LABORATORY
ATTN: TECHNICAL STAFF (PLS ROUTE)
DEPT. 5791
MS 0567, PO BOX 5800
ALBUQUERQUE, NM 87185-0567

SANDIA NATIONAL LABORATORY
ATTN: TECHNICAL STAFF (PLS ROUTE)
DEPT. 5704
MS 0655, PO BOX 5800
ALBUQUERQUE, NM 87185-0655

SANDIA NATIONAL LABORATORY
ATTN: TECHNICAL STAFF (PLS ROUTE)
DEPT. 6116
MS 0750, PO BOX 5800
ALBUQUERQUE, NM 87185-0750

AVI SHAPIRA
SEISMOLOGY DIVISION
THE INSTITUTE FOR PETROLEUM RESEARCH AND
GEOPHYSICS
P.O.B. 2286, NOLON 58122 ISRAEL

ROBERT SHUMWAY
410 MRAK HALL
DIVISION OF STATISTICS
UNIVERSITY OF CALIFORNIA
DAVIS, CA 95616-8671

DAVID SIMPSON
IRIS
1616 N. FORT MEYER DRIVE
SUITE 1050
ARLINGTON, VA 22209

BRIAN SULLIVAN
BOSTON COLLEGE
INSITUTE FOR SPACE RESEARCH
140 COMMONWEALTH AVENUE
CHESTNUT HILL, MA 02167

NAFI TOKSOZ
EARTH RESOURCES LABORATORY, M.I.T.
42 CARLTON STREET, E34-440
CAMBRIDGE, MA 02142

GREG VAN DER VINK
IRIS
1616 N. FORT MEYER DRIVE
SUITE 1050
ARLINGTON, VA 22209

TERRY WALLACE
UNIVERSITY OF ARIZONA
DEPARTMENT OF GEOSCIENCES
BUILDING #77
TUCSON, AZ 85721

JAMES WHITCOMB
NSF
NSF/ISC OPERATIONS/EAR-785
4201 WILSON BLVD., ROOM785
ARLINGTON, VA 22230

JIAKANG XIE
COLUMBIA UNIVERSITY
LAMONT DOHERTY EARTH OBSERVATORY
ROUTE 9W
PALISADES, NY 10964

OFFICE OF THE SECRETARY OF DEFENSE
DDR&E
WASHINGTON, DC 20330

TACTEC
BATTELLE MEMORIAL INSTITUTE
505 KING AVENUE
COLUMBUS, OH 43201 (FINAL REPORT)

MATTHEW SIBOL
ENSCO, INC.
445 PINEDA COURT
MELBOURNE, FL 32940

JEFFRY STEVENS
MAXWELL TECHNOLOGIES
P.O. BOX 23558
SAN DIEGO, CA 92123

DAVID THOMAS
ISEE
29100 AURORA ROAD
CLEVELAND, OH 44139

LAWRENCE TURNBULL
ACIS
DCI/ACIS
WASHINGTON, DC 20505

FRANK VERNON
UNIVERSITY OF CALIFORNIA, SAN DIEGO
SCRIPPS INSTITUTION OF OCEANOGRAPHY IGPP, 0225
9500 GILMAN DRIVE
LA JOLLA, CA 92093-0225

DANIEL WEILL
NSF
EAR-785
4201 WILSON BLVD., ROOM 785
ARLINGTON, VA 22230

RU SHAN WU
UNIVERSITY OF CALIFORNIA SANTA CRUZ
EARTH SCIENCES DEPT.
1156 HIGH STREET
SANTA CRUZ, CA 95064

JAMES E. ZOLLWEG
BOISE STATE UNIVERSITY
GEOSCIENCES DEPT.
1910 UNIVERSITY DRIVE
BOISE, ID 83725

DEFENSE TECHNICAL INFORMATION CENTER
8725 JOHN J. KINGMAN ROAD
FT BELVOIR, VA 22060-6218 (2 COPIES)

PHILLIPS LABORATORY
ATTN: XPG
29 RANDOLPH ROAD
HANSCOM AFB, MA 01731-3010

PHILLIPS LABORATORY
ATTN: GPE
29 RANDOLPH ROAD
HANSCOM AFB, MA 01731-3010

PHILLIPS LABORATORY
ATTN: TSML
5 WRIGHT STREET
HANSCOM AFB, MA 01731-3004

PHILLIPS LABORATORY
ATTN: PL/SUL
3550 ABERDEEN AVE SE
KIRTLAND, NM 87117-5776 (2 COPIES)